國立交通大學

光電工程研究所

碩士論文

利用同調多級光整流技術於硒化鎵晶體中產生兆赫輻射

Generation of terahertz radiation by coherent multiple-stage of optical rectification in GaSe crystals

研究生：林育賢

指導教授：潘犀靈　教授

安惠榮　教授

中華民國九十七年七月

利用同調多級光整流技術於硒化鎵晶體中產生兆赫輻射

Generation of terahertz radiation by coherent multiple-stage of optical rectification in GaSe crystals

研 究 生：林育賢　　Student： Yu-Shina Lin

指導教授： 潘犀靈　教授　　Advisors：Prof. Ci-Ling Pan

安惠榮　教授　　Prof. Hyeyoung Ahn

國 立 交 通 大 學

光電工程研究所

碩 士 論 文

A Thesis

Submitted to Institute of Electro-Optical Engineering

College of Electrical Engineering and Computer Science

National Chiao Tung University

In Partial Fulfillment of the Requirements

For the Degree of

Master of Engineering

In

Electro-Optical Engineering

July 2008

Hsinchu, Taiwan, Republic of China

中華民國九十七年七月

國　立　交　通　大　學

博碩士論文全文電子檔著作權授權書

（提供授權人裝訂於紙本論文書名頁之次頁用）

本授權書所授權之學位論文，為本人於國立交通大學光電工程系所＿＿＿＿組，96 學年度第二學期取得碩士學位之論文。

論文題目：利用同調多級光整流技術於硒化鎵晶體中產生兆赫輻射

指導教授：潘犀靈教授，安惠榮教授

■ 同意　□不同意

本人茲將本著作，以非專屬、無償授權國立交通大學與台灣聯合大學系統圖書館：基於推動讀者間「資源共享、互惠合作」之理念，與回饋社會與學術研究之目的，國立交通大學及台灣聯合大學系統圖書館得不限地域、時間與次數，以紙本、光碟或數位化等各種方法收錄、重製與利用；於著作權法合理使用範圍內，讀者得進行線上檢索、閱覽、下載或列印。

論文全文上載網路公開之範圍及時間：	
本校及台灣聯合大學系統區域網路	■ 中華民國98年8月28日公開
校外網際網路	■ 中華民國98年8月28日公開

授 權 人：林育賢

親筆簽名： 林育賢

中華民國 97 **年** 8 **月** 28 **日**

國　立　交　通　大　學

博碩士紙本論文著作權授權書

（提供授權人裝訂於全文電子檔授權書之次頁用）

本授權書所授權之學位論文，為本人於國立交通大學 光電工程 系所 ＿＿＿＿ 組，96 學年度第 二 學期取得碩士學位之論文。

論文題目：利用同調多級光整流技術於硒化鎵晶體中產生兆赫輻射

指導教授：潘犀靈教授，安惠榮教授

■ 同意

本人茲將本著作，以非專屬、無償授權國立交通大學，基於推動讀者間「資源共享、互惠合作」之理念，與回饋社會與學術研究之目的，國立交通大學圖書館得以紙本收錄、重製與利用；於著作權法合理使用範圍內，讀者得進行閱覽或列印。

本論文為本人向經濟部智慧局申請專利(未申請者本條款請不予理會)的附件之一，申請文號為：＿＿＿＿＿＿＿＿＿＿，請將論文延至＿＿年＿＿月＿＿日再公開。

授 權 人：林育賢

親筆簽名： 林育賢

中華民國 97 **年** 8 **月** 28 **日**

國家圖書館博碩士論文電子檔案上網授權書

ID:GT0095245350

本授權書所授權之論文為授權人在國立交通大學 電機 學院光電工程系所 組 96 學年度第 二 學期取得碩士學位之論文。

論文題目：利用同調多級光整流技術於硒化鎵晶體中產生兆赫輻射

指導教授：潘犀靈教授，安惠榮教授

茲同意將授權人擁有著作權之上列論文全文（含摘要），非專屬、無償授權國家圖書館，不限地域、時間與次數，以微縮、光碟或其他各種數位化方式將上列論文重製，並得將數位化之上列論文及論文電子檔以上載網路方式，提供讀者基於個人非營利性質之線上檢索、閱覽、下載或列印。

※ 讀者基於非營利性質之線上檢索、閱覽、下載或列印上列論文，應依著作權法相關規定辦理。

授權人：林育賢

親筆簽名： 林育賢

民國 97 **年** 8 **月** 28 **日**

國 立 交 通 大 學

論文口試委員會審定書

本校光電工程研究所碩士班 林育賢 君

所提論文 利用同調多級光整流技術於硒化鎵晶體中產生兆赫輻射

合於碩士資格標準、業經本委員會評審認可。

口試委員：趙如蘋 李晃逵

（趙如蘋 教授） （李晃逵 教授）

陳瓊華

（陳瓊華 教授）

指導教授：潘犀靈 安惠榮

所　　長：趙于飛 教授

系 主 任：黃中垚 教授

中 華 民 國 97 年 7 月 30 日

利用同調多級光整流技術於硒化鎵晶體中產生兆赫輻射

研究生：林育賢　　指導教授：潘犀靈 教授

安惠榮 教授

國立交通大學光電工程研究所

摘 要

本論文成功地建構一套理論模型以解釋非線性光學中光整流的機制行為。在考慮相位匹配參數及晶體的吸收係數的情況下，理論模擬利用超快雷射於硒化鎵晶體內光波混頻以產生兆赫輻射。而理論模擬於頻域上的光譜及時域上的波形的結果，可配合實驗數據來證實理論模型的正確性。進一步，將理論模型延伸於多級光整流的範疇，並檢視兆赫輻射於多級光整流情形下的同調機制與行為。

我們於實驗中利用多級光整流技術產生兆赫輻射，並透過調控兩級兆赫輻射之間的時間延遲關係，可以使兆赫輻射同調疊加並且擁有較高能量輸出，進一步證實此技術有應用於兆赫輻射任意波形調控的潛力。接著，利用光譜干涉法的分析方法，可得知兩級產生的兆赫輻射在不同的時間延遲下的同調關係在 1 THz 以下可達 0.8~0.95。另外，經由實驗結果擬合出兆赫輻射於硒化鎵晶體內的非線性吸收截面係數範圍約為$(1.3－5.9)\times10^{-17}$ cm^2。

多級光整流技術預期可以克服非線性晶體長度與晶體內群速度不匹配的限制，以同調串聯的方式產生高強度的兆赫輻射。經由理論模型計算的最佳化結果得知，使用超快雷射高脈衝能量產生經由多級光整流方式產生兆赫輻射的輸出可達 400.8 nJ。

Generation of terahertz radiation by coherent multiple-stage of optical rctification in GaSe crystals

Student: Yu-Shian Lin

Advisors: Prof. Ci-Ling Pan
Prof. Hyeyoung Ahn

Institute of Electro-Optical Engineering
College of Electrical Engineering and Computer Science
National Chiao Tung University

Abstract

In this thesis, we successfully construct a theoretical model to interpret the optical rectification process in nonlinear optics. Generation of terahertz radiation via frequencies mixing in GaSe crystal by use of the ultra-fast pulses laser is theoretically simulated by taking into account of the phase-matching parameter and absorption coefficient of nonlinear optical crystal. The frequency spectra and time-domain waveforms of terahertz radiation deduced from the numerical simulation are verified by the experimental results. Furthermore, this theoretical model can be extended to the application of coherent multi-stage optical rectification technique.

We experimentally generated terahertz radiation via multi-stage optical rectification process. By accurately adjusting the time delay between the two terahertz radiation from the two stages, the terahertz radiation can be coherently superposed with higher output power. This technique verifies the great potential of spectral synthesis of terahertz radiation. Moreover, it is observed that the coherence between the two terahertz radiation from the two stages is as high as 0.8~0.95 by the analysis of spectral-interfeometry method. Besides, the nonlinear absorption coefficient cross-section of GaSe crystal at terahertz frequencies is experimentally fitted in the range of $(1.3-5.9)\times10^{-17}$ cm^2.

Multi-stage optical rectification technique is expected to overcome the interaction length inside the nonlinear crystal, which is usually limited by group velocity mismatching. The high power terahertz radiation can be generated by coherently cascaded optical rectification processes in GaSe crystals. Under the numerical optimization, the single-cycle terahertz radiation can be generated with pulse energy as high as 400.8 nJ by use of the multi-stage optical rectification technique.

Acknowledgement

碩士班的日子飛快，從對超快研究領域懵懂未知的程度，到如今即將完成論文，真的讓我成長了許多。

首先要感謝我的指導教授潘犀靈教授，引領我進入兆赫波領域的研究，指出我實驗上的缺失以及指引研究方向。感謝我的共同指導安惠榮教授，在我碩士班研究過程中給予我鼓勵以及許許多多的建議。特別感謝遠從美國到來的嚴立教授，在我實驗進度中給予相當程度的建議以及方向，也幫助了我完成這份論文。感謝張振雄教授提供的晶體樣品以及李晃逵教授提供的雷射光源我才得以完成實驗。最需要感謝的是帶領我的 Moya 學長，不管在實驗上，程式上都給予我最大的助力，能完成本論文，學長當居首功。也感謝 Mika 學長對於雷射上的維護讓我得以有良好的實驗環境。在煩悶的時刻，能跟黎胖子鬼扯。另外和我一同奮鬥兩年的戰友，輝哥，阿 Ken，艾斯佛，一起修課，一起討論，也一起品嘗作研究的迷人與辛苦的地方，為我在平淡的研究生涯當中增添許許多多的色彩。良哥，choppy，山哥，阿駿，阿猛，幾位學弟的加入為實驗室增添樂趣。幾位學長學弟同學，認識的時光兩年的日子不長卻也不短，點滴銘刻在心。聚首的日子也所剩不多，有緣他日再會。

最後感謝我的母親給予我最大的支持，總是在我回家休息後，又有足夠動力去面對各式各樣的挑戰。

走過碩班兩年，經過不斷的嘗試與努力，涓涓細流到如今能有一點點的成果，都是有各位的幫助，願與各位共享。

Yu-Shian 2008/07 于風城

Contents

List of Figures

List of Tables

Chapter 1

Introduction to terahertz radiation

1.1 Background

Terahertz radiation (THz) is in the frequency range from about 0.1 to 10 THz, which corresponds to wave-numbers between 3 and 300 cm-1, photon energies between 0.4 and 40 meV, temperatures between 5 and 500 K and wavelengths between 3 mm and 30 μm. This frequency range, shown in the Fig.1-1, has several names: far infrared, sub-millimeter wave and terahertz range. The electromagnetic spectrum in this range is of great important due to the rich chemical and physical processes. For example, many materials have dominated properties in this spectrum range, such as the acceptor and donor in semiconductor, optical phonon properties, bang-gap of superconductor, vibrated or rotational energy level of most molecule, and the bonding energy of optical exciton. Compared to optical wave and X-ray, terahertz radiation has much smaller photon energy (4.1 meV). As a result, terahertz radiation is very suitable for application in the non-contacted measurement [1], and this kind of measurement can be used for bio-medical sciences and tissue inspections [2]. Terahertz imaging and tomography [3] have also been widely studied and could be applied to homeland security inspect. Even though terahertz radiation has great potential in various fields, it is unfortunate that this part of spectrum still has few difficulties and limitations for widely practical usage. Neither the terahertz radiation source is not easy to obtain nor the optical devices can not conveniently make work in the terahertz region because the terahertz frequency range locates between the

electronic and optical region of electromagnetic spectrum.

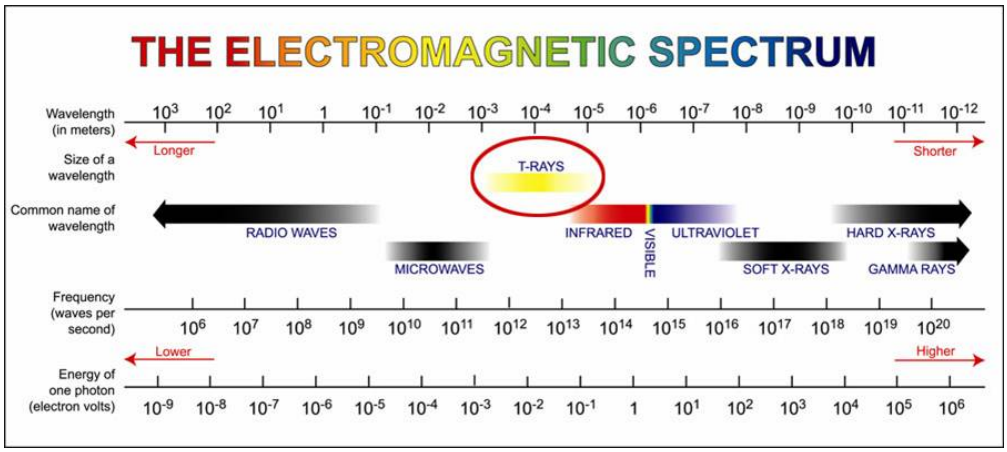

Fig.1-1 The spectrum range of electromagnetic waves.

The terahertz region of electromagnetic spectrum contained very poor light source, until the discovery of optical rectification and photo-conducting antenna. These two methods both provide stable radiation source and broad-band spectrum of terahertz wave. In the 1980s, the development of ultra-short pulsed laser make the research of terahertz radiation a great step forward. The ultra-short laser pulses about 100 femtosecond pulse duration is used as pump pulses that pass through the medium and create the electromagnetic pulses whose electric field is related to the intensity of pump light envelope of exciting pulses. The terahertz radiation generated normally contained few cycles of electric field in the near field, and both the amplitude and phase of their electric field can be measured. In 1980s, Auston [4] successfully used the photoconductive dipole antenna to generate and detect coherently terahertz radiation in time domain, and this technology is called terahertz time-domain spectroscopy (THz-TDS). Other terahertz radiation generation methods, such as optical rectification [5][6], surge current in semiconductor surface [7], had been investigated.

In 1995, X-C Zhang [8] successfully used ZnTe crystal to detect single cycle

terahertz radiation by free-space electro-optic sampling which highly increased the detection bandwidth and the signal to noise ratio (S/N ratio) up to 10^5 and achieved much large dynamic range. After that, a variety of the terahertz radiation generation methods are proposed by different mechanisms.

1.2 Overview of the GaSe crystal

Gallium Selenide is a semiconductor belongs to the III-VI layered semiconductor family, which has relatively large direct band gap of about 2.0 eV at room temperature. There are four polytypes of GaSe (β-, γ-, δ-, ε-type) classed by the package type of separate layers and their amount in the unit cell. The methods of growing ε-type GaSe are mainly the Bridgman-Stochbarger methods. Fig.1-2 shows the structure of ε-type GaSe crystal. The ε-GaSe consists of two layers and crystallizes with the space group ($P\bar{6}m2$), three anions form a tetrahedron along with the metal atom. The atoms are located in the planes normal to the c-axis in the sequence of Se-Ga-Ga-Se. Each layer consists of two planes of Ga atoms and surrounded by the unit planes of the Se atoms on two sides. Two sheets of the same layer are bonded with a mixture of covalent and ionic bonds, but the layers are hold by weak van der Waal's forces. Weakness of the interlayer binding of this single crystal gives rise to a strong anisotropy in the electrical properties. It is highly transparent in the infrared region between the wavelengths of 0.65-18 μm, is also a promising candidate material for nonlinear optical conversion devices in the near- to far-infrared. Besides the removal of the constraint of the lattice mismatch, GaSe thin film has the advantages of stability to against heating and oxidation under the ultra high vacuum condition. For practical application of nonlinear optics, the crystals should have promising properties. Such as large birefringence, high nonlinear coefficient, wide transparency range, low

absorption coefficient, and high damage threshold. GaSe has a wide transparency range from the wavelength of 0.62 to 18 μm with low optical absorption coefficient lower than 1 cm^{-1}. The ε-type is a negative uniaxial crystal which the ordinary refractive index is larger than extraordinary one. It has high nonlinear optical coefficients among the top five birefringent crystals. Due to its large birefringence, it can satisfy wide phase matching condition for different optical configurations within the nonlinear optical crystals. According to many promising properties in the far-infrared range, GaSe should be suitable to generate the terahertz radiation.

(a) (b)

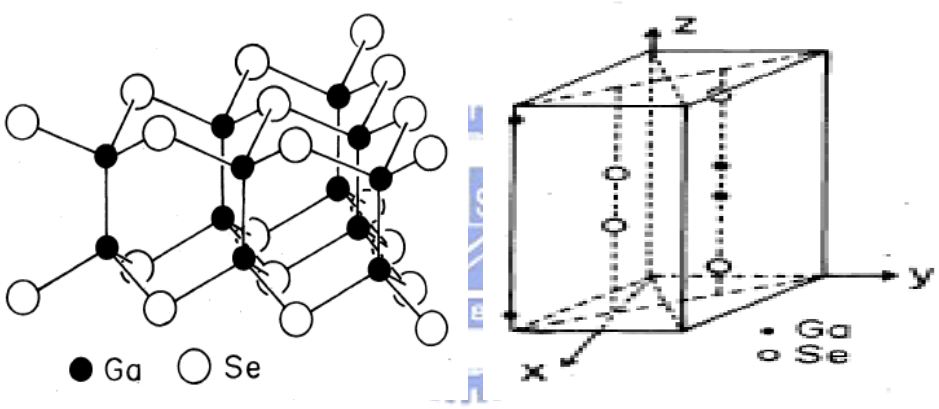

Fig.1-2 (a) The primitive layer of GaSe. (b) Unit cell of GaSe ε-type modification.

Nonlinear optical frequency mixing is a well known technique since the discovery of capability of the laser for generation of tunable coherent light using a single crystal. Recently, incoherent parametric super-radiant generation tunable in the range of 3.5–18 μm in GaSe (type-I PM) was obtained by using 110 ps pulses from the actively mode-locked Er:YAG laser as a pump source [9]. Subsequently, picosecond pulses of a mode-locked laser were used to pump a traveling-wave OPG; type-I and type-II OPG provided continuous tunability in the range of 3.5–14 and 3.9–10 μm, respectively [10]. On the other hand, there have been a number of reports

on difference frequency generation (DFG) to achieve tunable and coherent mid-infrared for GaSe by using variety of laser sources [11]. Additionally, few papers reported on the generation of far-infrared (THz wave) from GaSe crystal [12][13]. Moreover, GaSe has the largest figure of merit for the THz generation, which is several orders of magnitude large than that for bulk $LiNbO_3$ at 300 μm. According to Shi's results, an efficient and coherent THz wave tunable in the two extremely wide ranges of 2.7–38.4 and 58.2–3540 μm, with typical line-widths of 6000 MHz, had been achieved for the first time [14].

The nonlinear optical crystal is the heart of the nonlinear optical processes. There has been a lot of improvement in growth technology of nonlinear materials, particularly in the infrared region, and a number of nonlinear materials have been developed for laser device application. To perform efficiently, the material should possess a unique combination of optical, thermal and mechanical properties. The doping of the GaSe crystals was investigated to improve its optical and mechanical properties [15][16]. Recently, the electrical and optical characteristics of erbium doped GaSe (Er:GaSe) crystals had reported [17]. The two acceptor levels were found to originate either from the substitution of one Er^{3+} for one pair of Ga^{2+} or insertion of one Er^{3+} interstitial ions at interlayer sites in the unit cell. The structure of GaSe can also be slightly altered by the erbium doping. The optical properties of Er:GaSe crystals and its potential in the generation of mid-infrared radiation had been further explored [18].

In this work, the GaSe crystals were grown by a vertical Bridgman furnace. All the GaSe crystals used herein are home-made and provided by Prof. Chen-Shiung Chang's group from National Chiao Tung University (NCTU).

1.3 Laser system

The schematic of femtosecond laser system is shown in Fig.1-3. We use the Ti:Sapphire laser as the seeding laser which is then directed into the Ti:Sapphire regenerative amplifier for amplification. The pump laser of spectra physics Maitai laser is a 5W frequency doubled diode pumped Nd:YLF laser with a central wavelength at 532 nm. The Ti:Sapphire laser provides an output trace of intense 50 fs pulses with wavelength centered at 800 nm. The pulse repetition rate is 80 MHz and the output power could be up to 1.5 W.

The output beam of Maitai is used as seeding and guided into regenerative laser system (Hurricane Spectra-Physics). The seeding laser is stretched to avoid damaging the amplifier crystal. The pump laser for the amplification process in Hurricane is Q-switched Nd:YLF laser. This Nd:YLF laser delivers a high power output of 20 W at 527 nm. The amplified beam is then compressed to pulse width about 100 fs and output. The amplification process is called chirped pulse amplification shown in Fig. 1-4. The Hurricane amplifies the seeding pulses by a million times from few nano-Joule of energy per pulse to 0.7 milli-Joule per pulse. The pulse repetition rate is 1 KHz and the output power is about 700 mW.

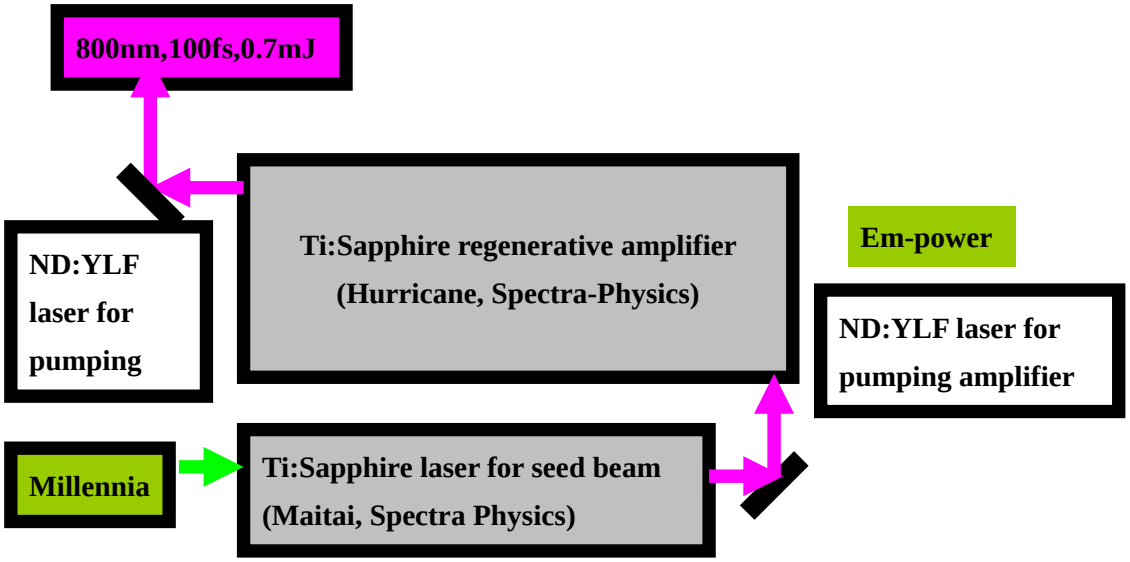

Fig.1-3 Femtosecond laser system includes Maitai, Hurricane and two pump laser (Millennia and Em-power)

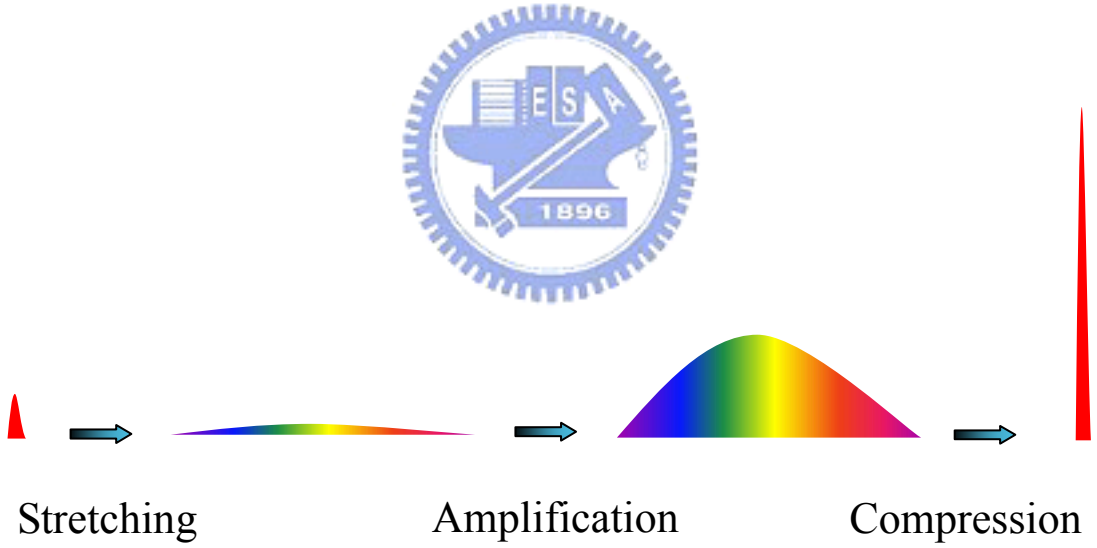

Fig.1-4 The chirped amplification process.

1-4 EO-sampling

When using THz-time domain spectroscopy system, (THz-TDS), the terahertz pulses are best detected via free space electro optic sampling, (FSEO sampling). The advent of the FSEO sampling method provide a new possibilities of high signal to

noise ratios and broad detection bandwidth of free space THz field. The premise behind FSEO sampling is the Pockels effect. In FSEO sampling, the terahertz pulse is generated and left to propagate through free space to the electro optic crystal. Fig. 1-5 shows the FSEO sampling scheme. A gate pulse is made to collinear with terahertz pulse after being sent through a time delay. This method allows the gating pulse to sample different parts of the terahertz field. Through the Pockels effect, the terahertz pulses change the refractive index and create the birefringence of the electro optic crystal. Thus the birefringence modifies the polarization of gating pulses. The most commonly used material for EO detection is ZnTe because of its relative large EO coefficient.

The Fig shows the geometry of FSEO sampling. The gating pulse and terahertz pulse are made to co-propagate into electro-optic crystal (e.g <110> ZnTe), and the birefringence modify the polarization of gating pulse, which should be initially be polarized at 45^{o} in order to obtain the maximum EO signal. After the EO crystal is quarter wave plate. The quarter wave plate provides a phase delay $\Gamma_0 = \frac{\pi}{2}$. Behind the quarter wave plate, the Wollaston prism follows, which separate the two polarization beam. The beam from the two outputs of the proceeding polarizing Wollaston prism are then incident onto balance detector.

The total phase change caused by the whole structure in refractive index could be expressed as a function of the electric field of terahertz pulses. The phase change equation for <110 ZnTe> is

$$\Gamma_{ZnTe} = \frac{2\pi}{\lambda} d n^3 \gamma_{41} E_{THz} \tag{1}$$

Where d is the thickness of the crystal, n is the refractive index of EO crystal at wavelength of gating beam, λ is the gating beam wavelength, γ_{41} is the EO

coefficient, and E_{THz} is the electric field of the terahertz wave. The only one varying variable is the applied field E_{THz}. The balanced detection signal for an FEO sampling could be calculated using Jones' matrices in combined with (1). The Jones matrix for ZnTe with phase delay between two principal polarizations is

$$J=\begin{pmatrix}\cos\frac{\pi}{4} & -\sin\frac{\pi}{4}\\ \sin\frac{\pi}{4} & \cos\frac{\pi}{4}\end{pmatrix}\begin{pmatrix}e^{i\delta} & 0\\ 0 & 1\end{pmatrix}\begin{pmatrix}\cos\frac{\pi}{4} & \sin\frac{\pi}{4}\\ -\sin\frac{\pi}{4} & \cos\frac{\pi}{4}\end{pmatrix}$$

Where $\delta=\Gamma_0+\Gamma$ is the phase delay between the two orthogonal coordinate of free space, containing the static term Γ_0 introduced by quarter wave plate, and dynamic term, induced by applied terahertz field.

Assuming the incident beam could be expressed as

$$\begin{pmatrix}E_x\\ E_y\end{pmatrix}e^{i\omega t}$$

.

Before the Wollaston prism, the electric field is

$$E(t)=\begin{pmatrix}\cos\frac{\pi}{4} & -\sin\frac{\pi}{4}\\ \sin\frac{\pi}{4} & \cos\frac{\pi}{4}\end{pmatrix}\begin{pmatrix}e^{i\delta} & 0\\ 0 & 1\end{pmatrix}\begin{pmatrix}\cos\frac{\pi}{4} & \sin\frac{\pi}{4}\\ -\sin\frac{\pi}{4} & \cos\frac{\pi}{4}\end{pmatrix}\begin{pmatrix}E_x\\ E_y\end{pmatrix}e^{i\omega t}$$

By using Jone's matrix operator, the output of electric field intensity of the two principal polarization of the ZnTe crystal are represented as

$$I_x=I_0\cos^2\frac{\Gamma+\Gamma_0}{2}$$

$$I_y=I_0\sin^2\frac{\Gamma+\Gamma_0}{2}$$

To separate the two principal polarization of output electric field intensity, the Wollaston prism is usually used. Generally, the Γ is usually small than 1($\Gamma<<1$),

thus we could take approximately solution

$$I_x = \frac{I_0}{2}(1-\Gamma)$$

$$I_y = \frac{I_0}{2}(1+\Gamma)$$

Through the balance detector, we measure the signal difference between I_x and I_y, so we could obtain final signal $I_0\Gamma$.

Combined with THz-TDS system, we could obtain the entire terahertz time domain waveform by measuring the signal difference between two beam intensity via balance detector as a function of time delay between terahertz pulse and gating pulse.

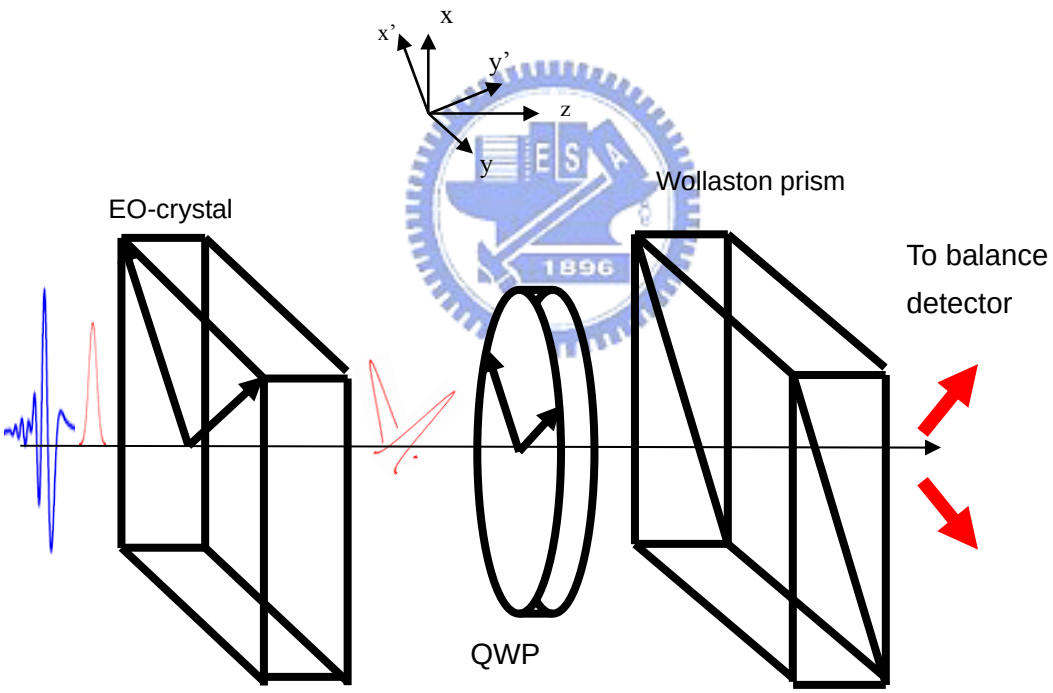

Fig.1-5 The scheme of EO sampling setup.

1.5 Motivation

GaSe crystal has been widely utilized to the generation and application of infrared and THz frequency regime. The conversion efficiency for generating the THz

radiation is usually quite low among the several promising techniques. In order to yields the intense single cycle and high amplitude THz wave, we propose a method to increase the output power of THz radiation. We propose the multiple stages of optical rectification technique which is useful for generating high amplitude single-cycle terahertz pulses, not limited by the pulse walk-off effect from group velocity mismatch in the nonlinear optical crystal used.

1.6 Organization of this thesis

In chapter 1, an overview of THz radiation and GaSe semiconductors are presented. In chapter 2, the basic principles of theories of terahertz radiation via optical rectification are described, both experimental and simulation results are included. In chapter 3, we demonstrate the superposition of the two terahertz in time domain , and the coherence of the terahertz wave is presented. In chapter 4, we introduce a method to generate higher power terahertz by superposition with high coherence and design a suitable condition to generate higher power terahertz. In chapter 5, the brief conclusion and summary are presented.

Reference

[1] D. Grischkowsky, Soren Keiding, Martin van Exter, and Ch. Fattinger, "Far-infrared time-domain spectroscopy with terahertz beams of dielectrics and semiconductors," J. Opt. Soc. Am. B, Vol. 7, No.10, pp. 2006-2015 (1990).

[2] M. Brucherseifer, M. Nagel, P. Haring Bolivar, and H. Kurz, "Lable-free probing of the binding state of DNA by time-domain terahertz sensing," Ultra. Pheno. Semi 2001, vol. 384, pp.253-258 (2002).

[3] B. B. Hu and M. C. Nuss, "Imaging with terahertz waves," Opt.Lett, vol.20, pp. 1716-1718 (1995).

[4] Auston D. H, Cheung. K. P. and Smith P R, "Picosecond photoconducting hertzian dipoles," Appl. Phys. Lett, vol.53, pp.1480-1482 (1988).

[5] X.-C. Zhang, Y. Jin, and X. F. Ma, "Coherent measurement of THz optical rectification from electro-optic crystals," Appl. Phys. Lett. **61**, 2764 (1992).

[6] A. Rice, Y. Jin, X. F. Ma, X.-C. Zhang, D. Bliss, J. Larkin, and M. Alexander, " Terahertz optical rectification from <110> zinc-blende crystals," Appl. Phys. Lett. 64, 1324 (1994).

[7] X.-C. Zhang and D. H. Auston, "Optoelectronic measurement of semiconductor surface and interface with femtosecond optics," J. Appl. Phys, vol.71, pp.326-338 (1991).

[8] Q. Wu, and X. -C. Zhang, "Free-space electro-optic sampling of terahertz beams," Appl. Phys. Lett. 67, 3523-3525 (1995).

[9] Wei Shi Ding, Y.J. Xiaodong Mu Fernelius, N. ," Tunable and coherent radiation in the range of 2.7-29 um based on difference-frequency generation in GaSe,**"** Appl. Phys. Lett. 80**,** 3889 (2002).

[10] K. L. Vodopyanov and V. G. Voevodin, "2.8 μm laser pumped type I and type II travelling-wave optical parametric generator in GaSe," Optics Communications, vol. 14, No.3-4, pp.333-335.

[11] K. L. Vodopyanov, "Parametric generation of tunable infrared radiation in ZnGeP2 and GaSe pumped at 3μm," Opt. Soc. Am. B Vol. 10, No.9 (1993).

[12] K. Liu, J. Xu, and X. C. Zhang, "GaSe crystals for broadband terahertz wave detection," Appl. Phys. Lett. 85, 863-865 (2004).

[13] T. Tanabe, K. Suto, J. -i. Nishizawa, and T. Sasaki, "Characteristics of terahertz-wave generation from GaSe crystals," J. Phys. D: Appl. Phys. 37, 155-158 (2004).

[14] Wei Shi, Yujie J. Ding, Nils Fernelius, and Konstantin Vodopyanov, " Efficient, tunable, and coherent 0.18–5.27-THz source based on GaSe crystal," Optics Letters, Vol. 27, Issue 16, pp. 1454-1456 (2002)

[15] S. Das, C. Ghosh, O.G. Voevodina, Yu.M. Andreev and S.Yu. Sarkisov, “Modified GaSe crystal as a parametric frequency converter,” Applied Physics B: Lasers and Optics, Vol.82, No.1 (2005).

[16] D. R. Suhre, N. B. Singh, V. Balakrishna, N. C. Fernelius, and F. K. Hopkins, ” Improved crystal quality and harmonic generation in GaSe doped with indium,” Optics Letters, Vol. 22, Issue 11, pp. 775-777 (1997).

[17] Yu-Kuei Hsu and Chen-Shiung Chang, “Electrical properties of GaSe doped with Er,” J. Appl. Phys. 96, 1563 (2004).

[18] Yu-Kuei Hsu, Ching-Wei Chen, Jung Y. Huang, Ci-Ling Pan, Jing-Yuan Zhang, and Chen-Shiung Chang, ”Erbium doped GaSe crystal for mid-IR applications,” Optics Express, Vol. 14, No.12, pp. 5484-5491.

Chapter 2

Overview of optical rectification

2.1 Background

Optical rectification is the second-order of nonlinear process in which the D.C frequency (comparing to optical frequency range) of electric field is produced by intense optical pump illumination in the nonlinear medium [1]. Due to the development of picosecond and femtosecond pulsed laser, currently, generating ultrashort, single cycle THz electromagnetic pulses via optical rectification is much easier.

Generally, optical rectification refers to the generation of a DC polarization via an intense optical pulse. Most optical electric field strength, even with a laser sources, are small compared with characteristic crystalline chemical bonding. Therefore, the electronic polarization could be expanded in the powers series of the driving electric force.

$$\tilde{P}^{(nl)} = \varepsilon_0[\chi^{(2)}\tilde{E}\tilde{E} + \chi^{(3)}\tilde{E}\tilde{E}\tilde{E} + \chi^{(4)}\tilde{E}\tilde{E}\tilde{E}\tilde{E} + higher\ order\ term] \qquad (1)$$

The nonlinear susceptibility of $\chi^{(n)}$ is the tensor of n order of n+1 rank. The second order polarization is the lowest term, which could yield a DC contribution. In general, the individual tensor components will depend on the frequencies fields involved.

Terahertz optical rectification is induced by an intense pump pulses. More accurately, the terahertz optical rectification should be considered as nearly degenerate difference frequency generation with each frequency pair in a single cycle optical pulse. When a pump pulse containing broadband spectrum, which is

dominated by the pulse shape and the pump pulse duration, is incident into the nonlinear EO crystal, the nonlinear interaction between two frequency components will induce a nonlinear polarization at the beating frequency.

Considering the lowest order of nonlinear interaction, the second order polarization for optical rectification is with the form:

$$\tilde{P}^{(2)}(\omega_T) = \varepsilon_0 \chi^{(2)}(\omega_T; \omega_p + \omega_T, -\omega_p)\tilde{E}(\omega_p + \omega_T)\tilde{E}^*(\omega_p) \quad (2)$$

$\chi^{(2)}$ is the second order susceptibility, third rank tensor which of $3\times3\times3$ components. Symmetry determines which of the tensor components are vanished and which components are equal. For second order nonlinear interaction, the material must possess non-central symmetry. For broadband pump pulses, the electric field in equation (2) contains the frequencies $\omega_p + \omega_T$ and ω_p. The ω_T is the DC frequency far from optical range. For convenience, we take the effective nonlinearity $d_{eff} = \frac{1}{2}\chi_{eff}$ in replace of the susceptibility. The DC polarization, $\tilde{P}^{(2)}(\omega_T)$, and the amplitude, $E(\omega)$, of the applied optical electric field at frequency ω_T has the form:

$$P^{(2)}(\omega_T) = 2d_{eff}E(\omega + \omega_T)E^*(\omega) \quad (3)$$

Under the phase matching condition, the field of the beating frequency radiation has a continuous spectrum with frequency as high as several terahertz and corresponding waveforms.

2.2 Theory of optical rectification

The one-dimensional equation for the Fourier component of the THz field at the angular frequency, ω_T, $E_T(\omega_T)$, could be derived directly from the Maxwell's equations.

$$\nabla \bullet \tilde{E}(z,t) = 0 \tag{4}$$

$$\nabla \times \tilde{E}(z,t) = \frac{d}{dt}\tilde{B}(z,t) \tag{5}$$

$$\nabla \bullet \tilde{B}(z,t) = 0 \tag{6}$$

$$\nabla \times \tilde{H}(z,t) = \tilde{J} + \frac{d}{dt}\tilde{D}(z,t) \tag{7}$$

By double curl operator and constitution relation, the wave equation could be recast into

$$\nabla(\nabla \bullet \tilde{E}(z,t)) - \nabla^2 \tilde{E}(z,t) = -\mu_0 \frac{d}{dt}\sigma \tilde{E}(z,t) - \mu_0 \varepsilon_0 \frac{\partial^2}{\partial t^2}\tilde{E}(z,t) - \mu_0 \frac{\partial^2}{\partial t^2}\tilde{P}^{(nl)}(z,t) \tag{8}$$

where ε_0 and μ_0 are the permittivity and permeability in free space, respectively, and σ is the conductivity. In addition, $\tilde{E}$ and $\tilde{P}$ expresses the time varying electric field and polarization. It is assumed that the medium is with no free current, so that the first term of right handed side is vanished, and we drop the first term of left handed side by the reason of assuming the medium is without free charges.

$$\nabla \bullet \tilde{D}(z,t) = 0 \tag{9}$$

Therefore, the wave equation could be simplified as follow:

$$-\nabla^2 \tilde{E}(z,t) = -\mu_0 \varepsilon_0 \frac{\partial^2}{\partial t^2}\tilde{E}(z,t) - \mu_0 \frac{\partial^2}{\partial t^2}\tilde{P}^{(nl)}(z,t) \tag{10}$$

Herein, the plane wave analysis is applied, the electric field and the nonlinear polarization are the linear combination of different frequency:

$$\tilde{E}(z,t) = \sum_n E_n(\omega_n, z)e^{-i\omega_n t} \tag{11}$$

$$\tilde{P}(z,t) = \sum_n P_n(\omega_n, z)e^{-i\omega_n t} \tag{12}$$

here

$$E_n(\omega_n, z) = E_n(\omega_n)e^{ik_n z} \tag{13}$$

$$P_n^{nl}(\omega_n, z) = P_n^{nl}(\omega_n)e^{ik_n z} \tag{14}$$

When the relations above are introduced into Eq.(10), a wave equation analogous to Eq.(10) is obtained. The wave equation valid for each frequency component of the field is shown as follows:

$$-\nabla^2 E_n(\omega_n, z) = -\mu_0 \varepsilon_0 \omega_n^2 E_n(\omega_n, z) - \mu_0 \omega_n^2 P^{(nl)}(\omega_n, z) \tag{15}$$

2.3 Terahertz wave generation by optical rectification

Under the strong pump, the pump pulse is almost constant in propagating.

$$\frac{d}{dz}E_p(\omega, z) \Rightarrow E_p(\omega, z) \sim const \tag{16}$$

This implies that the pump is non-depleted. This physical assumption makes us consider terahertz generation only. Under the slowly varying envelope approximation:

$$\frac{\partial^2}{\partial z^2}E_n(\omega_n, z) << i2k_n \frac{d}{dz}E_n(\omega_n, z) \tag{17}$$

and in the limit of no absorption $\alpha = 0$, the terahertz generation could be expressed as follow:

$$\frac{d}{dz}E_T(\omega_T, z) = \frac{i\mu_0 \omega_T^2}{2k_T(\omega_T)}P^{(nl)}(\omega_T, z) \tag{18}$$

where the Fourier components of the nonlinear polarization, $P^{(nl)}(\omega_T, z)$, could be expressed through the material effective nonlinearity d_{eff} as:

$$P_T^{nl}(\omega_T, z) = 2\varepsilon_0 d_{eff} \int E_p(\omega + \omega_T, z)E_p^*(\omega, z)e^{i\Delta k_T z} d\omega \tag{19}$$

where $E_T(\omega_T, z)$ and $E_p(\omega, z)$ denote the terahertz radiation field and the optical pump field, respectively. The k-vector mismatch Δk_T is given by the following

relation [2][3]:

$$\Delta k_T = k(\omega_p + \omega_T) - k(\omega_p) - k(\omega_T) \tag{20}$$

and the d_{eff} for the crystal of GaSe for type-oee phase matching is given by the handbook as follows [4]:

$$d_{eff} = d_{22}\cos^2(\theta)\cos(3\varphi) \tag{21}$$

The differential equation Eq.(19) is terahertz generation via optical rectification described the second order nonlinear optical process. The phase matching determine the whether $E_T(\omega_T, z)$ could be generated. The others linear coefficients dominate the amplitude strength of the generated field.

Consider an optical pump, broad bandwidth-limited ultrashort (e. g, femtosecond) laser pulses propagating along z in the form of infinite plane waves with the Gaussian time envelope profile of the electric field. In simulation, we assume that the incident pump light pulse has a Gaussian temporal shape as:

$$e_p(0,t) = E_0 e^{-2\ln 2\frac{t^2}{\delta t^2}} \tag{22}$$

$$E_p(0,t) = \mathrm{Re}\{e_p(0,t)e^{-i\omega_0 t}\} \tag{23}$$

where ω_0 is the central frequency of optical pump, and δt is the pulse width, which is defined by the full width at half maximum of the intensity of pulse shape. Under the Fourier transform limit, the pump light pulse could be expressed as:

$$e_p(z,t) = \int E_p(\omega, z)e^{ik_0 z}e^{-i\omega t}d\omega \tag{24}$$

The Fourier transform of the incident optical wave at z=0 becomes:

$$E_p(\omega,0) = \frac{E_0\delta t}{2\sqrt{2\pi\ln 2}}e^{-\frac{\delta t^2(\omega-\omega_0)^2}{8\ln 2}} \tag{25}$$

where $E_p(\omega)$ is a one-sided $(\omega > 0)$ Fourier components.

Similar one-sided Fourier representation will be used for other fields below in the text. For arbitrary z,

$$E_p(\omega, z) = E_p(\omega)e^{ik_p(\omega)z} \tag{26}$$

where $k_p(\omega)$ is the wave vector of pump pulse.

2.4 Parameters of GaSe

We use the parameters of GaSe crystal as the electro-optical medium. The central wavelength of the pump pulse is treated as 800 nm. The dielectric function in terahertz range and Sellmeier equation in optical range are introduced by [5]. Dispersion of the GaSe crystal in terahertz region is described by a complex dielectric function at angular frequency, ω:

$$\varepsilon_o(\omega) = A\omega^6 + B\omega^4 + C\omega^2 + S_1 + \frac{(\omega_L^2 - \omega_T^2)S_1}{\omega_T^2 - \omega^2 - i\Gamma_1\omega} + \frac{\omega_t^2 S_2}{\omega_t^2 - \omega^2 - i\Gamma_2\omega} \tag{27}$$

$$\varepsilon_e(\omega) = A'\omega^6 + B'\omega^4 + C'\omega^2 + S_3 + \frac{(\omega_L^2 - \omega_T^2)S_3}{\omega_T^2 - \omega^2 - i\Gamma_3\omega} \tag{28}$$

In optical region, the refractive index $n(\lambda)$ for ordinary and extraordinary optical wave are shown as derived from Sellmeier equation, respectively:

$$n_o^2 = A + \frac{B}{\lambda^2} + \frac{C}{\lambda^4} + \frac{D}{\lambda^6} + \frac{E\lambda^2}{\lambda^2 - F} + \frac{G\lambda^2}{\lambda^2 - H} \tag{29}$$

$$n_e^2 = A' + \frac{B'}{\lambda^2} + \frac{C'}{\lambda^4} + \frac{D'}{\lambda^6} + \frac{E'\lambda^2}{\lambda^2 - F'} \tag{30}$$

here λ represents the wavelength in μm. The parameters of each equation are list in the table 2-1.

	Ordinary ε_o									
Parameter	A (cm^6)	B (cm^4)	C (cm^2)	S_1	S_2	Γ_1 (cm^{-1})	Γ_2 (cm^{-1})	ω_L (cm^{-1})	ω_T (cm^{-1})	ω_t (cm^{-1})
Value	6.105×10^{-27}	1.856×10^{-18}	4.049×10^{-9}	7.37	0.017	2.8	0.566	255	213.5	19.53

	Extraordinary ε_e						
Parameter	A' (cm^6)	B' (cm^4)	C' (cm^2)	S_3	Γ_3 (cm^{-1})	ω_L (cm^{-1})	ω_T (cm^{-1})
Value	122.3×10^{-27}	-22.88×10^{-18}	3.879×10^{-9}	5.76	2.8	245.5	237

	Parameter	Value		Parameter	Value
n_o	A	7.37	n_e	A'	5.76
	B	0.405		B'	0.3879
	C	0.0186		C'	-0.2288
	D	0.0061		D'	0.1223
	E	3.1436		E'	0.4206
	F	2193.8		F'	1780.3
	G	0.017			
	H	262177.5577			

Table 2-1 Parameters of Sellmeier equation dielectric function.

2.5 Simulation result

$\boxed{\Delta k_T = 0 \quad \text{and} \quad \alpha_T = 0}$

First, here we conduct numerical simulation under conditions of perfect phase matching ($\Delta k_T = 0$) and without absorption ($\alpha_T = 0$). On the other hand, we neglect the pump-depleted effect. It is assumed that the pump pulse is not changed with propagating, in order to understand the basic physical nature of the optical rectification process.

The power spectrum of terahertz and corresponding waveform obtained by the calculation are shown in Fig.2-1(a) as a function of the propagation length inside GaSe crystal from 0 to 2mm. the terahertz spectrum grows almost linearly as a function of the propagation length, and a little change in the shape change in the shape is observed.

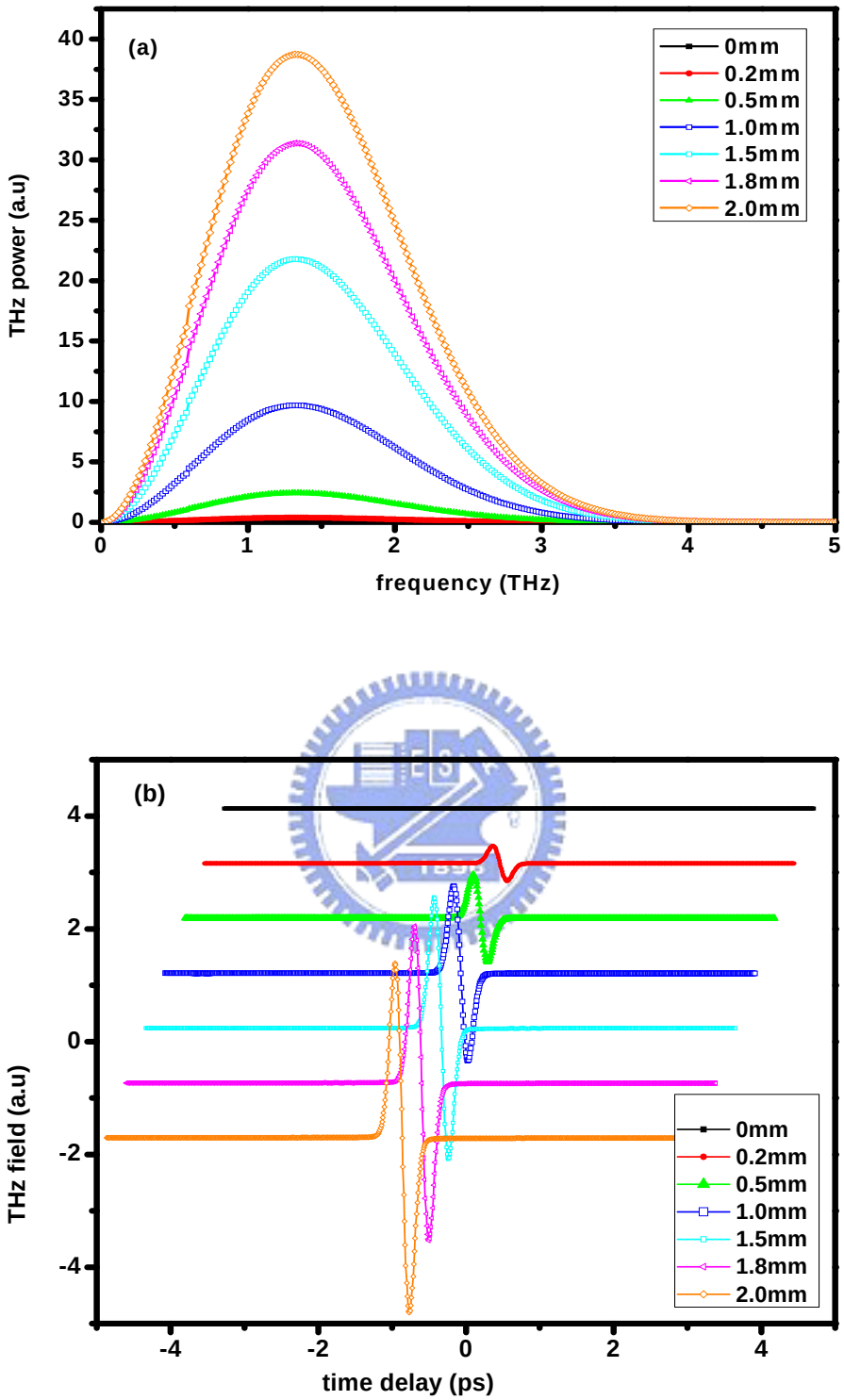

Fig.2-1 (a) Power spectra of THz under perfect phase matching and no absorption condition at propagation distances in the GaSe crystal form 0 to 2mm. (b) Temporal waveforms of THz field obtained corresponding to the same

condition.

The temporal waveform of the terahertz pulses are displayed in Fig. 2-1(b). The waveforms are almost proportional to the second order time derivative of the pump pulse shape in this figure. Although the assumption of no change in the pump field is the simulation condition, in very low conversion efficiency the results we obtain from numerical calculation study is still adoptable and predictable.

$\boxed{\Delta k_T \neq 0 \quad \text{and} \quad \alpha_T = 0}$

Now we examine the effects of real phase condition on the terahertz optical rectification processes by finite phase mismatching, $\Delta k_T \neq 0$. Similarly, we keep the absorption as zero. Parameters of the pump pulses are the same as that in the previous case. Terahertz spectrum obtained by simulations is shown in Fig.2-2(a) as a function of propagation length. The peak of the terahertz spectrum is not linearly growing, and the spectral bandwidth becomes narrower as the propagation length increases due to the fast varying phase matching condition. As the propagating length increasing, the spectrum peaks shift to lower frequency. It is noticed that the spectrum with a deep around 0.58 THz is due to the absorption of transverse optical phonon [2].

Temporal waveform of the terahertz radiation is shown in the Fig.2-2(b). It could be observed that the dispersion relation causes the oscillation tailoring and make the terahertz waveform broadened.

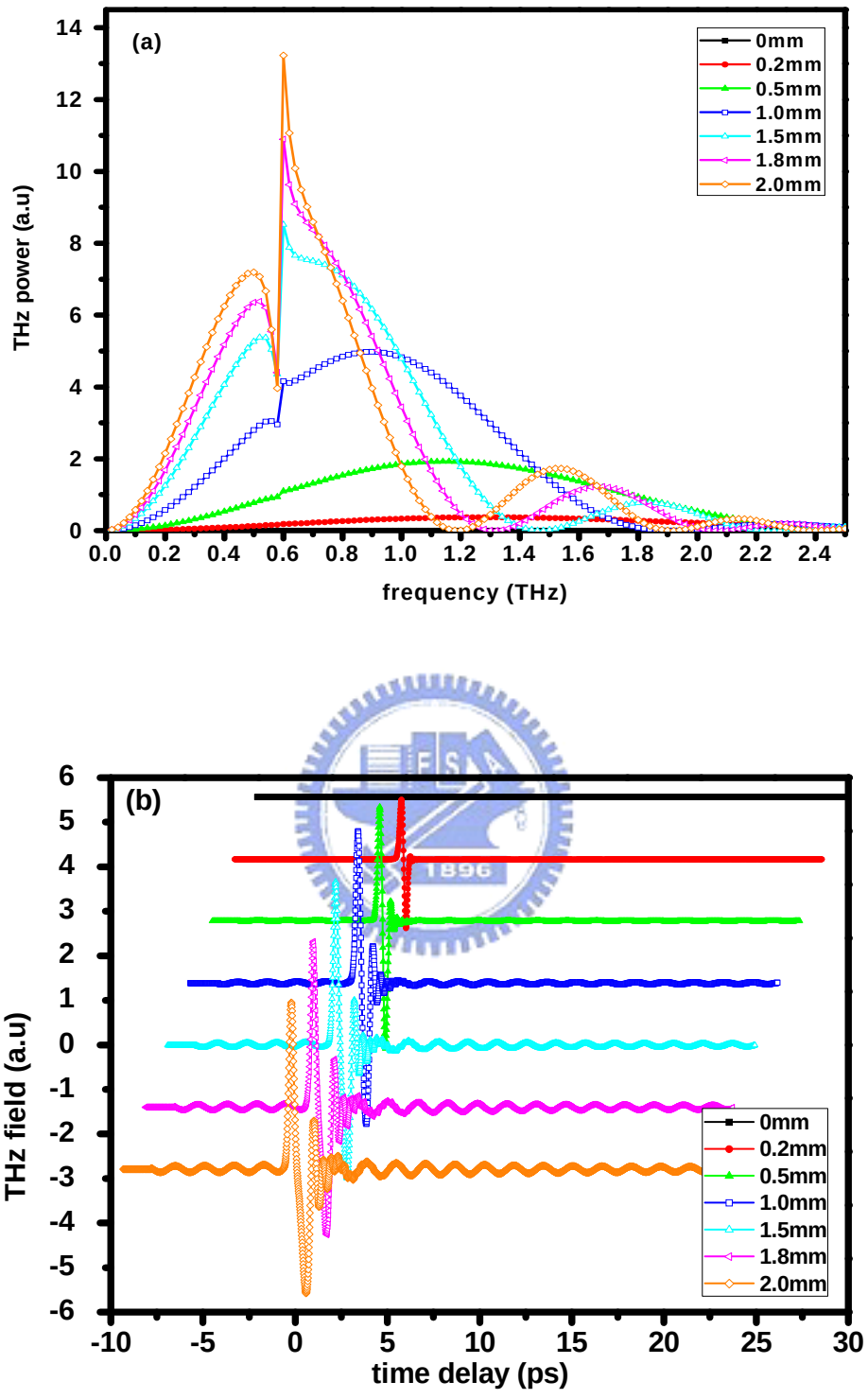

Fig.2-2 (a) Power spectra of THz under realistic phase mismatches and no absorption conditions at propagation distances in the GaSe crystal from 0 to 2mm. (b) Temporal waveforms of THz pulses corresponding to same conditions.

$\boxed{\Delta k_T \neq 0 \text{ and } \alpha_T \neq 0}$

The frequency dependent absorption effect is included in this case. The absorption coefficient α_T in terahertz range is as a function of frequency. The absorption coefficient is defined as:

$$\alpha_{\mathrm{T}} = \frac{4\pi}{\lambda}\kappa(\omega) \tag{30}$$

where κ is the imaginary part of refractive index derived from dielectric function in terahertz range.

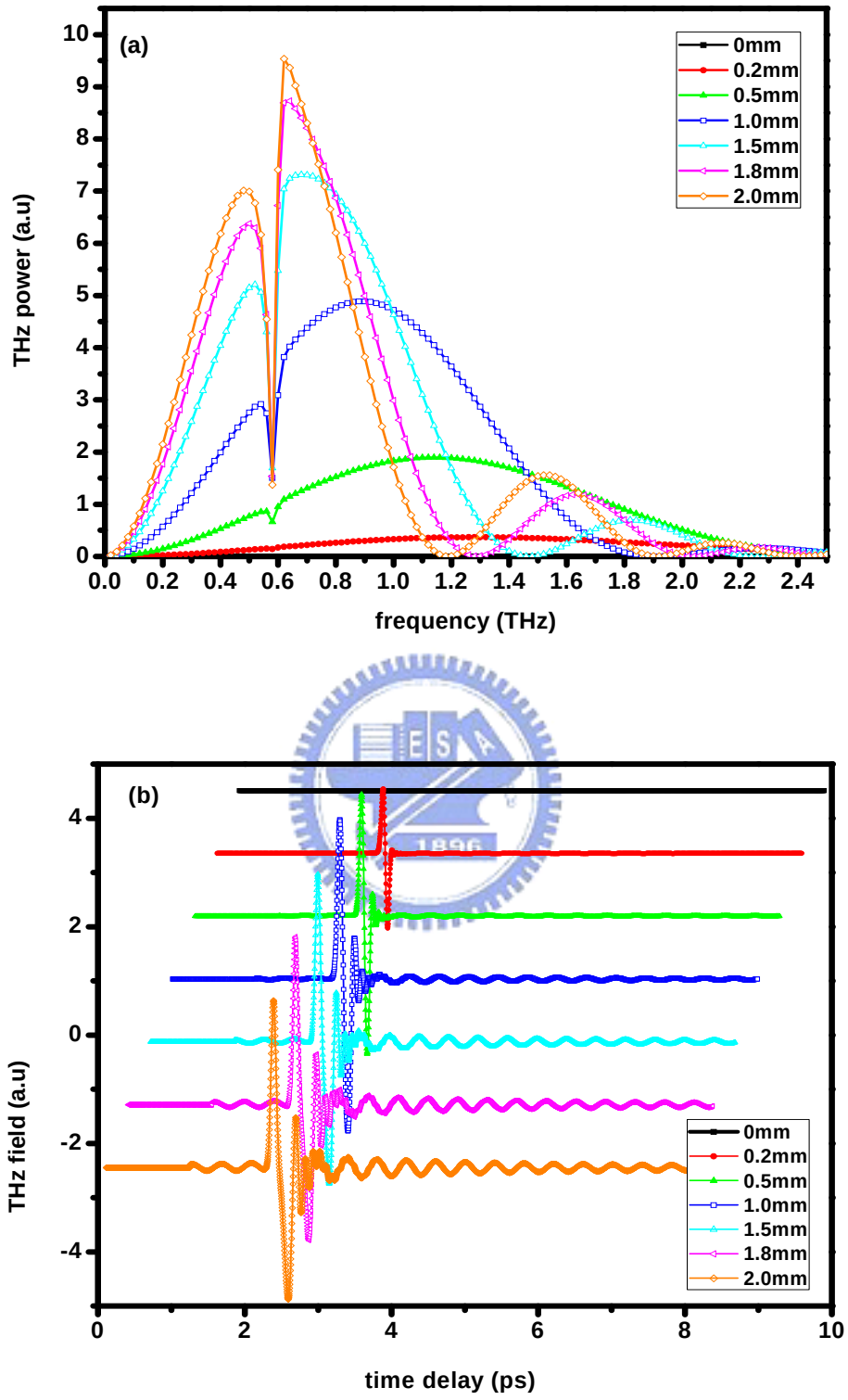

Fig.2-3 (a) Power spectra of THz under realistic phase mismatches and absorption along propagating distances in the GaSe crystal from 0 to 2mm. (b)Temporal waveforms of THz pulses corresponding to same conditions.

2.6 Experimental results

The experimental setup for terahertz generation by optical rectification is shown in Fig.2-4. The optical pump source utilizes a Ti: sapphire laser with a 1-kHz repetition rate. The pulse energy is about 700 μJ, central wavelength at 800 nm, with 280 fs pulse duration. The beam splitter reflects 10% of input power as THz-TDS gating pulse, transmits 90% as terahertz pump source.

Terahertz radiation is generated from 2 mm GaSe crystal. Fig.2-5 shows the geometry of terahertz radiation via GaSe crystal by optical pump pulse. The residual laser beam are blocked by Teflon and terahertz wave are passed through wire-grid polarizer to make sure the polarization, then terahertz wave are guided by four parabolic mirrors to ZnTe crystal [6]. The indium-tin-oxide (ITO) glass plate, which transmit the optical pump pulse while partially reflects the terahertz pulse, is used as the terahertz dichroic mirror reflecting terahertz between second and third parabolic mirror. A pellicle beam splitter which is transparent to the terahertz beam and has a reflectivity of 5% for optical pump pulse is used to combine terahertz pulse and gating pulse and make the gating pulse collinear with the terahertz pulse into ZnTe crystal. For monitoring the time-domain waveform of terahertz radiation, we employed the electro-optical sampling technique with a 1 mm thick ZnTe crystal. The terahertz pulse and gating pulse co-propagate through ZnTe crystal. The linear polarization of the gating beam is perpendicular to the polarization of the terahertz pulse. The azimuthal angle of ZnTe could be adjusted to obtain maximum E-O signal. The linear polarization of the gating pulse without been modulated by the terahertz pulse is converted to circular polarization by quarter wave plate. Polarization of the gating pulse modulated by the terahertz pulse is converted to ellipsoid polarization by a quarter wave plate. Behind the quarter wave plate, the Wollaston prism follows, and

separates the modulated ellipsoid polarized gating pulse into two orthogonal polarizations, *s*- and *p*-polarization. Both polarizations are guided to balance detector. The electrical signal of balanced detector is connected to a lock-in amplifier in order to increase the signal to noise ratio (S/N ratio). An optical chopper is used in this experimental arrangement to modulate the optical pump beams for optical rectification of terahertz radiation.

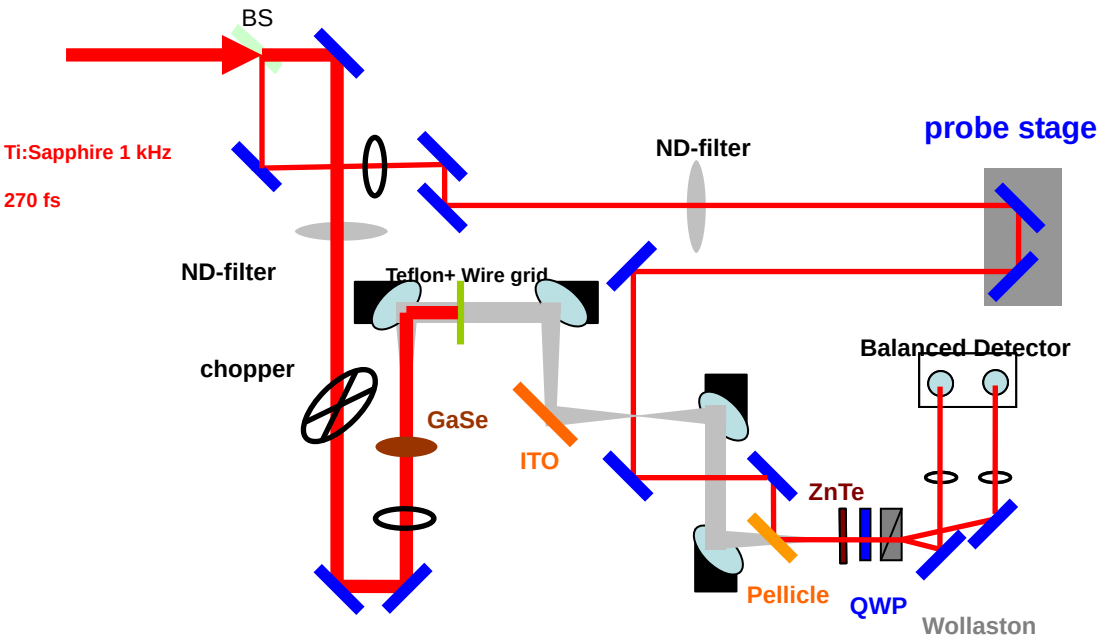

Fig.2-4 The experimental setup of electro-optic THz system.

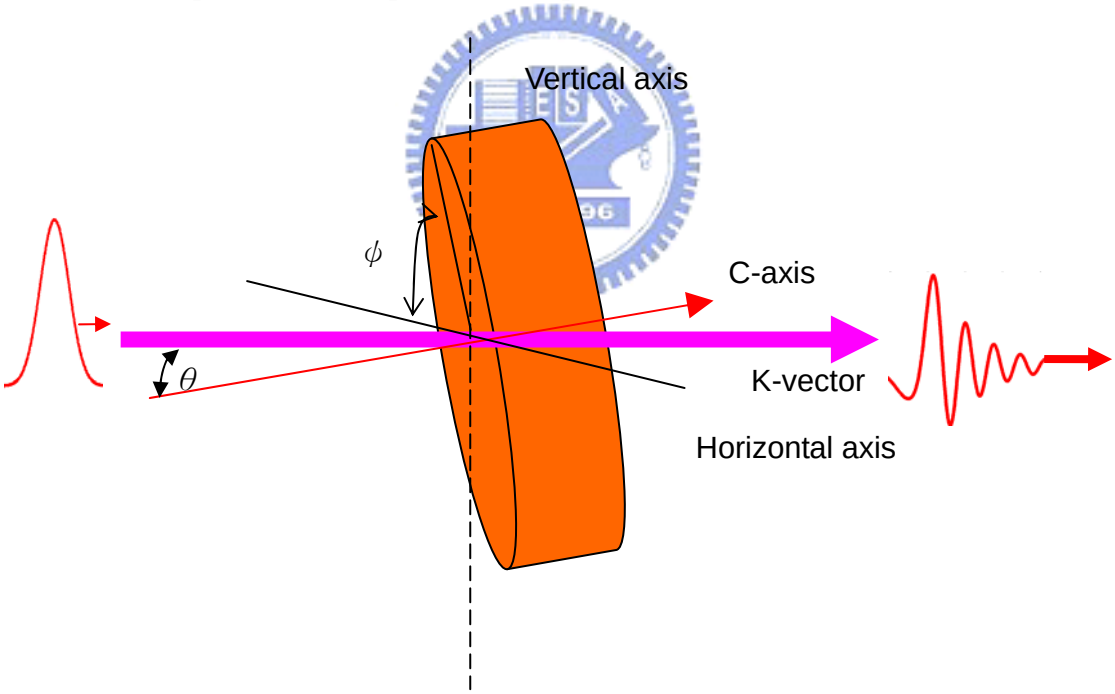

Fig.2-5 The scheme of THz generation via optical rectification in GaSe crystal.

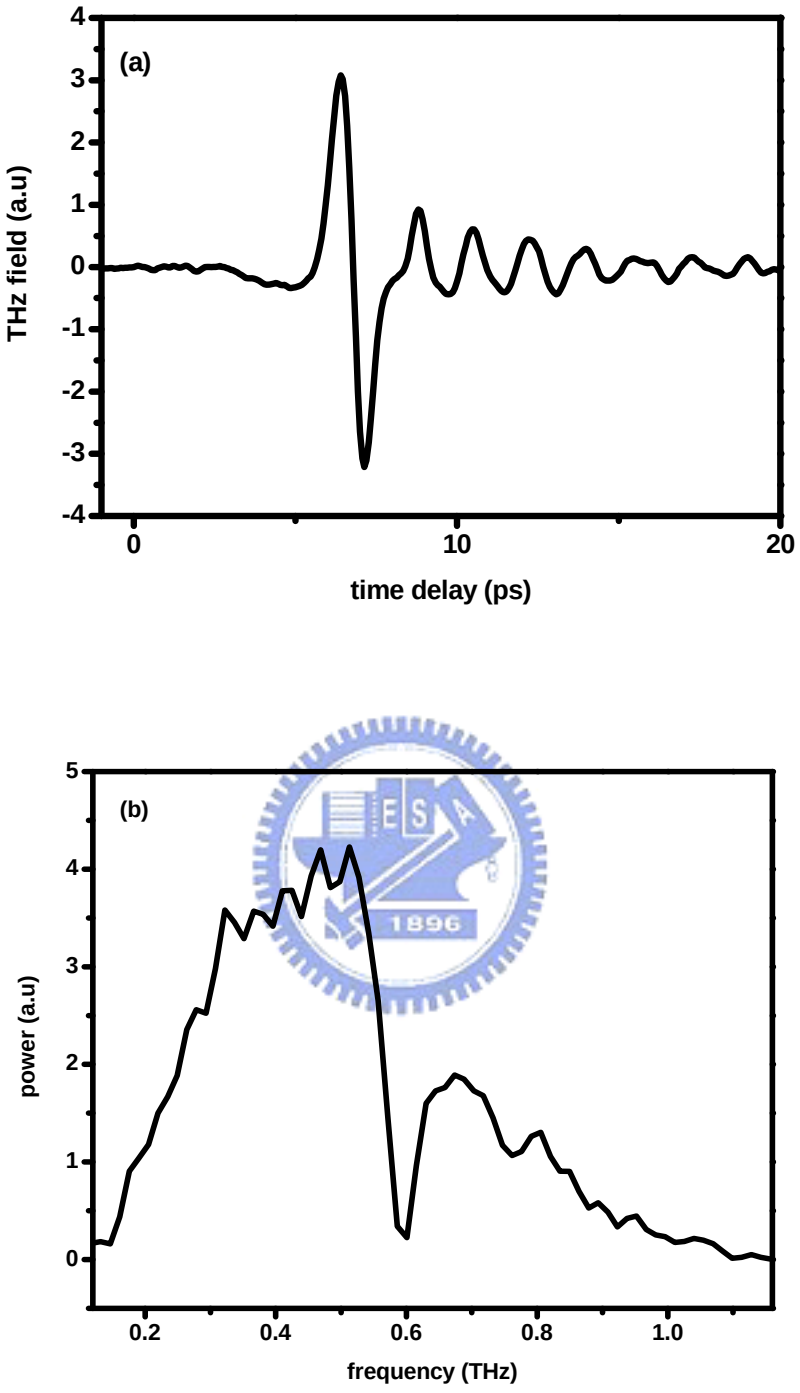

Fig. 2-6 (a) THz electric field profile in the time domain via EO sampling detection.

(b) Power spectrum versus frequency of the THz pulse in (a)

Fig.2-6(a) shows the terahertz radiation time domain waveform and corresponding spectrum from GaSe crystal. The terahertz spectrum is also with a deep around 0.58 THz agreed well with simulation result, also corresponds to the absorption of transverse optical phonon of dielectric function.

2.7 Effective nonlinearity

Optical rectification is nonlinear optical behavior related to the second-order susceptibility. THz output from the OR is dependent on the value of the nonlinearity d_{eff}. The d_{eff} of the GaSe crystal is expressed as follows:

$$E_{THz} \propto d_{eff} = d_{22} \cos^2 \theta \cos 3\varphi \tag{31}$$

By selecting the suitable φ angles, THz peak electric field and the d_{eff} could be optimized. Fig.2-7 shows the THz time domain waveforms at different GaSe azimuthal φ angle. This relationship is attributed to the hexagonal crystal symmetry in the uniaxial crystal. It has been shown that the maximum signal is achieved when the GaSe emitter has its azimuthal angle set at $|\cos 3\varphi| = 1$, since the effective nonlinear coefficient of type-II phase matching is proportional to the value of cos3φ. Fig.2-8 presents the THz wave peak amplitude versus azimuthal φ angle for GaSe emitter.

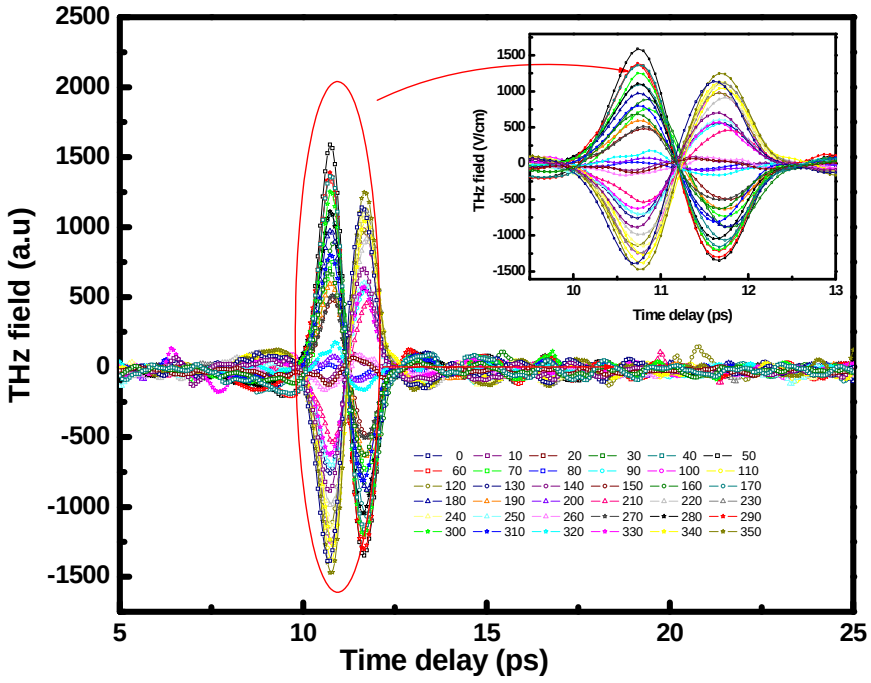

Fig.2-7 THz time domain waveforms at different azimuthal angle.

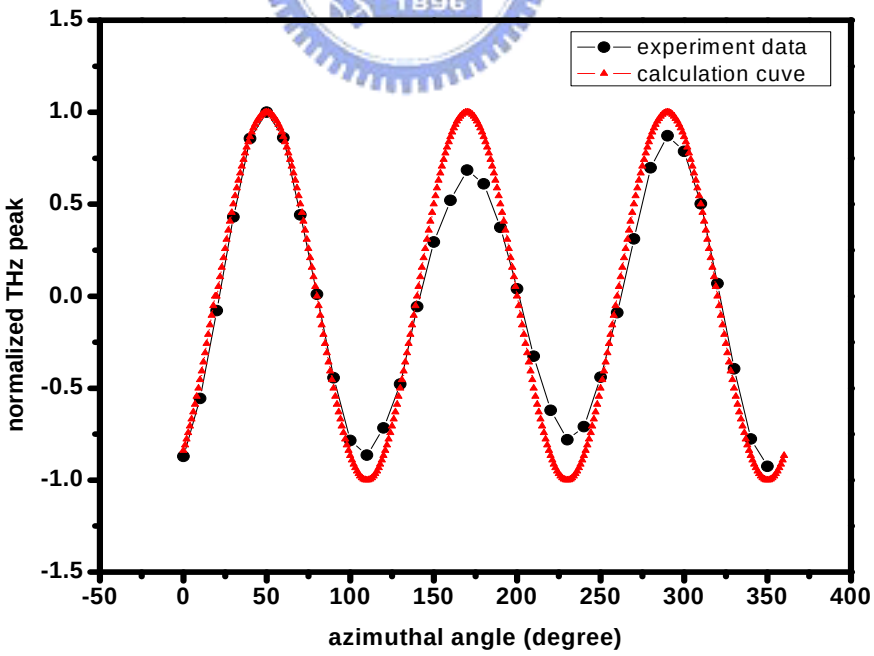

Fig.2-8 THz wave peak amplitude versus azimuthal angle for GaSe emitter.

2.8 Summary

We demonstrated the numerical simulations based on one dimensional terahertz generation by optical rectification in GaSe crystal which possesses the large nonlinearity suitable for terahertz generation. Effects of perfect phase matching and no absorption, and also realistic phase matching and absorption conditions are also discussed by use of the parameter of GaSe crystal. The numerical simulation results of several cases show that the phase matching condition could have a significant effect on the optical rectification processes for terahertz pulse generation despite the dispersion of the EO medium.

Reference

[1] A. Nahata, A.S. Weling, T.F. Heinz, “A wideband coherent terahertz spectroscopy system using optical rectification and electro-optic sampling,” Appl. Phys. Lett. 69, 2321 (1996)

[2] Y. R.Shen, “The principle of nonlinear optics, 1st edition”.

[3] R. E. Boyd, “Nonlinear optics, 2nd edition”.

[4] E. D. Palik, Handbook of Optical Constants of Solids (Academic, New York, 1998), Vol. III.

[5] Ching-Wei Chen, Tsung-Ta Tang, Sung-Hui Lin, Jung Y.Huang, Chen-Shiung Chang, Ci-Ling Pan, Pei-Kang Chung, Shun-Tung Yen, “Optical properties and potential applications of ε-GaSe crystal in terahertz frequencies,” prepared to submit.

[6] Q. Wu, and X. -C. Zhang, “Free-space electro-optic sampling of terahertz beams,” Appl. Phys. Lett. 67, 3523-3525 (1995).

Chapter 3

Superposition and coherence in multiple stages of optical rectification

3.1 Theoretical model

The nonlinear interacting processes between the optical and terahertz pulses in cascaded GaSe multiple stages optical rectification could be properly described with the coupled wave equations. Under the slowly varying envelope approximation, the one dimensional coupled propagation equations [1] are derived as

$$\frac{d}{dz}E_P(\omega_P,z)=j\frac{\mu_0\varepsilon_0 d_{eff}\omega_P^2}{k_p(\omega_P)}\int E_P(\omega_P-\omega_{T,2},z)E_T(\omega_{T,2},z)e^{i\Delta k_P z}d\omega_{T,2}-\frac{\alpha_P}{2}E_P(\omega_P,z) \quad (1)$$

$$\frac{d}{dz}E_{T,2}(\omega_{T,2},z)=j\frac{\mu_0\varepsilon_0 d_{eff}\omega_{T,2}^2}{k_T(\omega_T)}\int E_p(\omega_p+\omega_{T,2},z)E_P^*(\omega_P,z)e^{i\Delta k_{T,2} z}d\omega_P-\frac{\alpha_{T,2}}{2}E_{T,2}(\omega_{T,2},z) \quad (2)$$

Here z is the propagation distance in GaSe crystal, E_P and E_T denote the terahertz radiation field and the optical pump pulse in the second stage, respectively; ε_0 and μ_0 are permittivity and permeability in free space, respectively; d_{eff} is effective nonlinearity; ω_P and ω_T are angular frequencies of optical pump pulse and terahertz pulse; α_P and $\alpha_{T,2}$ are the linear absorption coefficients of optical pump pulse and terahertz pulse in second GaSe; the Δk_P and $\Delta k_{T,2}$ denote the wave vector phase mismatches.

The total terahertz field in time domain could be described by

$$E_T(\omega_T)=E_{T,1}(\omega_T)e^{-i\omega_{T,1}\tau}+E_{T,2}(\omega_T) \quad (3)$$

where $E_{T,1}$ and $E_{T,2}$ are the terahertz radiation fields from the first and second optical rectification stage, respectively; τ expresses the propagation time delay of the two stage optical rectification stage.

3.2 The minimum variance distortionless response

Here we used a method of minimum variance distortionless response (MVDR), it is used in spectral estimation. And we used this approach to estimate the cross-spectrum and magnitude squared coherence function (MSC) function. First, we calculated cross spectrum. By using the cross spectrum, we analyzed the coherence of each frequency between the two terahertz radiations.

Let $x(n)$ be a time varying signal, which is the input of K filters of length L, $g_k = [\, g_{k,0}\ g_{k,1}\ \cdots\ g_{k,\text{L-1}}\ ]^{\text{T}}$, $k = 0,1\cdots K-1$. The superscript T denotes transpose. If we denote the $y_k(n)$ as the output signal of the filter function of g_k, its power is shown as:

$$E\{|y_k(n)|^2\} = E\{|g_k^H x(n)|^2\} = g_k^H R_{xx} g_k \tag{4}$$

where $E\{\bullet\}$ expresses the expectation value, and superscript H expresses the transpose conjugate of a vector, and R_{xx} is defined as:

$$R_{xx} = E\{x(n)x^H(n)\} \tag{5}$$

here R_{xx} is the covariance matrix of the input signal $x(n)$. In this analysis, we assume that R_{xx} is positive definite.

Consider the $(L \times K)$ matrix,

$$F = [\, f_0\ \cdots\ f_k \cdots f_{K\text{-}1}\,],\ \ k = 0,1,2\cdots K-1 \tag{6}$$

Here

$$f_k \frac{1}{\sqrt{L}}[1\ e^{j\omega_k}\ \cdots\ e^{j\omega_k(L\text{-}1)}]^T, \text{ and } \omega_k = \frac{2\pi k}{K} \tag{7}$$

The F matrix is called the Fourier matrix and be unitary. This implies $F^H F = FF^H = I$. In the MVDR spectrum, the filter coefficients are chosen so as to minimize the variance of the filter output, subject to the constraint:

$$g_k^H f_k = f_k^H g_k = 1 \tag{8}$$

Under the Eq. (8), the signal $x(n)$ is passed through the filter g_k without distortion at frequency ω_k, and signals at other frequencies tend to be attenuated. This expression could be described by mathematical model:

$$J_k = g_k^H R_{xx} g_k + \mu[1 - g_k^H f_k], \tag{9}$$

and μ is Lagrange coefficient. The minimization of Eq. (9) lead to a solution [2]:

$$g_k = \frac{R_{xx}^{-1} f_k}{f_k^H R_{xx}^{-1} f_k} \tag{10}$$

According to the Eq. (10), we obtain the spectrum of $x(n)$ at frequency ω_k as:

$$S_{xx}(\omega_k) = E\{|y_k(n)|^2\} = E\{|g_k^H x(n)|^2\} = g_k^H R_{xx} g_k. \tag{11}$$

Applying Eq. (10) into Eq. (11), we get $S_{xx}(\omega_k) = \frac{1}{f_k^H R_{xx}^{-1} f_k}$.

Replacing Eq. (10), we obtain

$$R_{xx} g_k = S_{xx}(\omega_k) f_k. \tag{12}$$

For all vectors of f_k, the Eq. (12) has a general form

$$R_{xx}\mathbf{G} = \mathbf{F}\mathbf{S}_{xx}(\omega), \quad \mathbf{G} = [g_0\ \ g_1 \cdots\ g_k \cdots g_{K\text{-}1}] \tag{13}$$

and

$$\mathbf{S}_{xx}(\omega) = diag\{S_{xx}(\omega_0)\ \ S_{xx}(\omega_1) \cdots S_{xx}(\omega_{K\text{-}1})\} \tag{14}$$

which is a diagonal matrix.

Assuming here that the two signal $x_1(n)$ and $x_2(n)$ with respective spectra $S_{x_1x_1}(\omega_k)$ and $S_{x_2x_2}(\omega_k)$. We could design a function

$$g_{j,k} = \frac{R_{x_jx_j}^{-1} f_k}{f_k^H R_{x_jx_j}^{-1} f_k}, \quad j = 1,2, \tag{15}$$

to find the spectra of $x_1(n)$ and $x_2(n)$ at frequency ω_k

$$S_{x_jx_j}(\omega_k) = \frac{1}{f_k^H R_{x_jx_j}^{-1} f_k}, \quad j = 1,2, \tag{16}$$

Where $R_{x_jx_j} = E\{x_p(n)x_p^H(n)\}$ is the covariance matrix of the signal $x_p(n)$ and

$$\mathbf{x}_p(n) = [\, x_p(n) \;\; x_p(n\text{-}1) \;\; \cdots x_p(n\text{-}L+1) \,]^T \tag{17}$$

If we let $y_{1,k}(n)$ and $y_{2,k}(n)$ be the respective output of the function $g_{1,k}$ and $g_{2,k}$, we could get the cross-spectrum between $x_1(n)$ and $x_2(n)$ at frequency ω_k as

$$S_{x_1x_2}(\omega_k) = E\{y_{1,k}(n)y_{2,k}^*(n)\} \tag{18}$$

Here the super script * denote the complex conjugate.

For the same method, we could get

$$S_{x_2x_1}(\omega_k) = E\{y_{2,k}(n)y_{1,k}^*(n)\} = S_{x_1x_2}^*(\omega_k) \tag{19}$$

If we develop Eq. (19), we get

$$S_{x_1x_2}(\omega_k) = g_{1,k}^H R_{x_1x_2} g_{2,k}, \tag{20}$$

Here $R_{x_1x_2} = E\{\mathbf{x}_1(n)\mathbf{x}_2^H(n)\}$ is the cross-correlation matrix between $x_1(n)$ and $x_2(n)$.

To obtain the cross-correlation spectrum, we apply Eq. (15) into Eq. (20):

$$S_{x_1x_2}(\omega_k) = \frac{f_k^H R_{x_1x_1}^{-1} R_{x_1x_2} R_{x_2x_2}^{-1} f_k}{[\, f_k^H R_{x_1x_1}^{-1} f_k \,][\, f_k^H R_{x_2x_2}^{-1} f_k \,]} \tag{21}$$

3.3 Magnitude squared coherence (MSC) function

According cross-correlation spectrum, we define the magnitude squared coherence (MSC) function between two signals $x_1(n)$ and $x_2(n)$ as [3],

$$\gamma^2_{x_1x_2}(\omega_k) = \frac{\left|S_{x_1x_2}(\omega_k)\right|^2}{S_{x_1x_1}(\omega_k)\, S_{x_2x_2}(\omega_k)} \tag{22}$$

So from Eq. (21), the magnitude squared cross correlation spectrum is:

$$\left|S_{x_1x_2}(\omega_k)\right|^2 = \frac{\left| f_k^H R^{-1}_{x_1x_1} R_{x_1x_2} R^{-1}_{x_2x_2} f_k \right|^2}{[\, f_k^H R^{-1}_{x_1x_1} f_k\,]^2\ [\, f_k^H R^{-1}_{x_2x_2} f_k\ ]^2}. \tag{23}$$

Using the expressions of Eq. (16) and Eq. (23) into Eq. (22), The MSC function becomes:

$$\gamma^2_{x_1x_2}(\omega_k) = \frac{\left| f_k^H R^{-1}_{x_1x_1} R_{x_1x_2} R^{-1}_{x_2x_2} f_k \right|^2}{[\, f_k^H R^{-1}_{x_1x_1} f_k\,]\,[\, f_k^H R^{-1}_{x_2x_2} f_k\ ]} \tag{24}$$

3.4 Experiment setup and result

The used laser system is a 1k-Hz amplified Ti:sapphire laser with pulse energy of $700\,\mu J$ and pulse duration of 280 femtosecond. The experimental setup for multi-stage optical rectification is shown in Fig. 3-1. The first beam splitter reflects 10% of input power as gating beam, and the second beam splitter reflects 60% for first terahertz generation and transmitted 40% for second terahertz generation. The typical average pump power on the GaSe crystals is about 130mW and 150mW for the first and second stage respectively. The pump beam diameter for both stages is adjusted to be about 3 mm. Both GaSe crystals are configured for non-phase matched optical rectification. The terahertz radiation field generated from the first optical rectification stage of 2-mm thick GaSe crystal is guided into the second stage of 3-mm thick GaSe. Again we block the residual optical pump laser with Teflon plates terahertz wave are passed through wire-grid polarizer to make sure the polarization. The terahertz pulse

from the two OR stages are aligned collinearly with two gold-coated parabolic mirrors and guided into ZnTe crystal. The time delay between the two terahertz pulses are carefully controlled with a translation stage. The optical chopper is used in this experimental arrangement to simultaneously modulate the optical pump beams for the first and second OR stage. Also the electro-optical sampling technique with a 1-mm thick ZnTe crystal is used. Terahertz radiation generated from either the first or second stage, or both could be recorded without moving any optical element.

By adjusting the terahertz pulses from the two GaSe optical rectification stages to temporally overlap. The optical path length of the pump pulse to the first GaSe stage is then varied to adjust the arrival time of the terahertz pulse at the second GaSe stage.

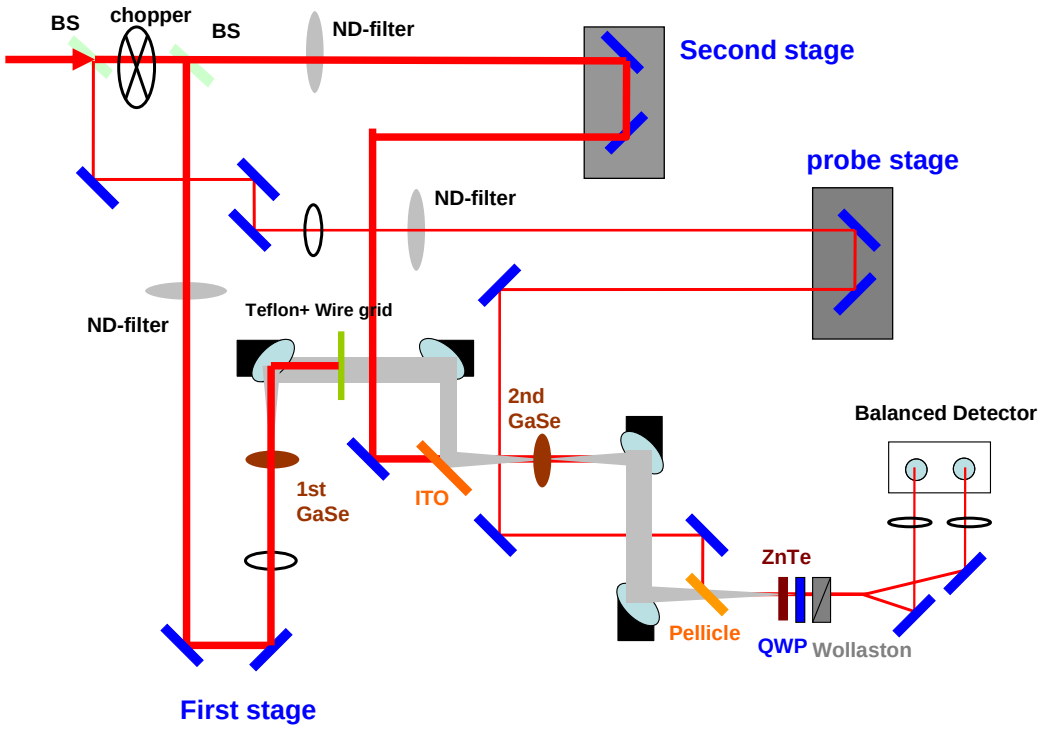

Fig.3-1 Schematic of coherent generation of terahertz radiation by multi-stage optical rectification in GaSe crystals. BS: Beam splitter; ND-Filter: Neutral Density filter; ITO: indium-tin-oxide glass plate; λ/4: quarter wave plate.

Figure 3-2 shows the time domain field amplitude of the terahertz output from the second OR stage as a function of the arrival time of the seeding terahertz field. In this case, the terahertz field generated in the second stage is added to the incoming THz seeding field. We can also map out the seeding terahertz pulse profile by scanning the first stage delay line while blocking the pump pulse to the second GeSe crystal. The resulting first terahertz pulse profile was shown as the square-symbols in Fig. 3-2. High degree of mutual coherence between the terahertz fields from the two GaSe OR stages was clearly revealed.

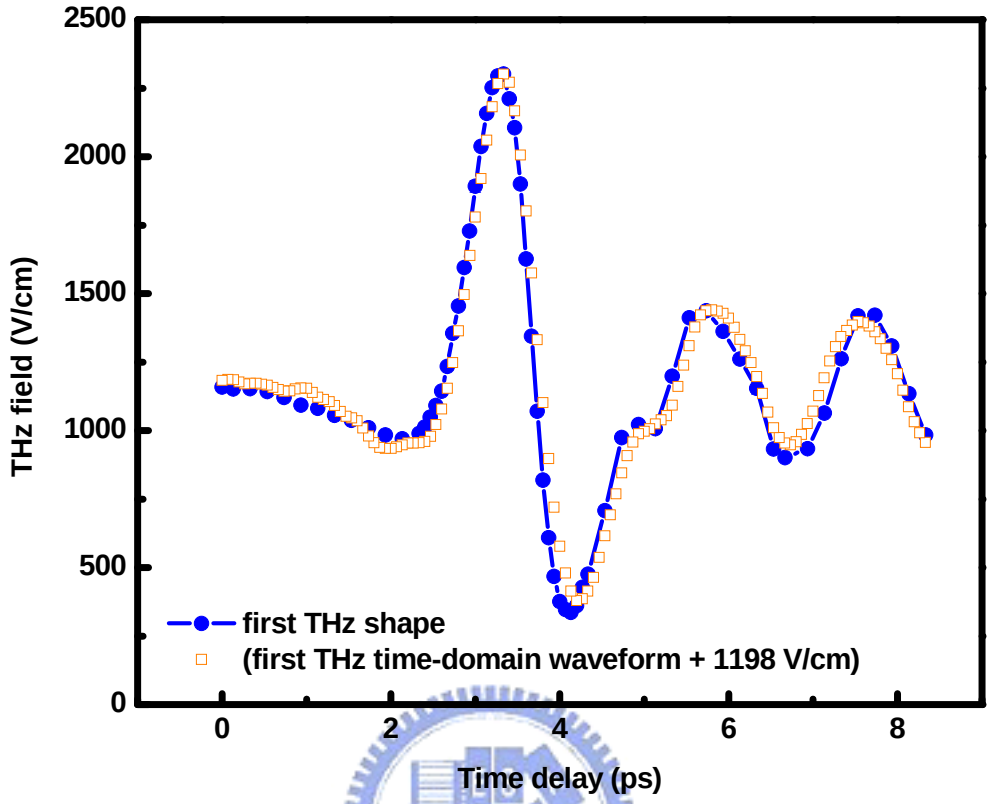

Fig. 3-2 Terahertz field amplitude after the second stage is plotted as a function of arrival time of the seeding THz pulse. Dot-symbols present the terahertz output from the second OR stage. Square-symbols represent the first terahertz time-domain waveform from the first stage, which is scaled for the easy comparison with output from the second stage.

Figure 3-3 shows the terahertz time-domain waveforms and the spectra at three different time delays between the two OR stages. In these figures, the signal from the first stage is presented as black dashed curve and the pulse from the second stage is displayed with the red dashed-dot line. The superposed THz pulses from both stages are shown as the blue curve with open squares. By adjusting the time delay, the terahertz fields from the two OR stages can be superposed constructively or

destructively. To generate maximum terahertz field, the time delay of the two terahertz pulses should be adjusted for the best temporal overlap within 0.1 ps in our study, to yield constructive superposition over the entire spectral components involved.

In Fig. 3-3(a), the main peak of terahertz field from the second OR stage leads that from the first stage. However, the trailing part of the THz pulse from the second stage still overlaps and interferes with the THz field from the first stage. The coherent superposition nature is more clearly revealed in the frequency domain shown in the inset of the Fig. 3-3(a). Parts of the terahertz spectral components from the two stages are constructively added to produce higher spectral power while some spectral regions superpose destructively to yield lower spectral power. Thus the coherent superposition with multiple terahertz radiation sources offers a potential for the synthesis of terahertz field. In Fig. 3-3(c), the terahertz pulse from the second stage lags behind that from the first stage in such a way that the main positive peak from the second stage overlaps with the negative amplitude of the THz pulse from the first stage. The destructive superposition yields a spectrum shown in the inset of Fig. 3-3(c). The destructive superposition is caused by out-of-phase mixing of the terahertz field from the first stage with the optical pump pulse in the second OR stage. The spectral phase content of the terahertz field can then be imprinted onto the pump pulse. In other words, when pump pulse in the second OR stage and terahertz field from the first stage are getting close and partly overlapped in the time domain, the seeding terahertz field will dominate the three-wave mixing process and lead to the output terahertz field profile variations. In the case of Fig. 3-3(c), the phase difference almost equals to π in the overlapped region between terahertz field from the first stage and the pump pulse in the second OR stage. Thus the terahertz field generated by the

pump pulse in the second OR stage is then superposed with the first THz field to yield a much weaker terahertz radiation output.

The highest terahertz field amplitude can be obtained by synchronizing the first and second OR stages to attain constructive superposition of terahertz fields in the second OR stage. This can be done by seeding terahertz field with the correct phase at a proper arrival time relative to the optical pump pulse of the second stage. The output terahertz field possesses the property of the seeding terahertz field but with higher amplitude. The inset of Fig. 3-3(b) presents the spectra of the terahertz radiation fields to reveal the amplification nature of terahertz radiation pulse after the coherent superposition of the two stages.

The terahertz signal measured by the electro-optical sampling technique could be affected by the dispersion of the terahertz signal; the velocity-matching condition between the terahertz and optical pulses, and non-perfect alignment. The theoretical simulation of the two OR stages with Eqs. (1)-(3) is performed in order to remove the artifacts in the practical experiment. To allow for a straightforward comparison of the THz spectral profile with the measured data, we assume a non-transform limited optical pump pulse with a spectral width < 1 THz. The absorption by the optical phonon mode of GaSe at 0.58 THz was also included in our simulation. The calculation results corresponding to the three different experimental conditions are presented in Figs. 3-3(d), 3(e), and 3(f). The simulation results agree well with the experimental data shown in Figs. 3-3(a), (b) and (c), respectively. This confirms that the theoretical model used to depict the coherent multi-stage optical rectification processes in GaSe crystals is satisfactorily accurate.

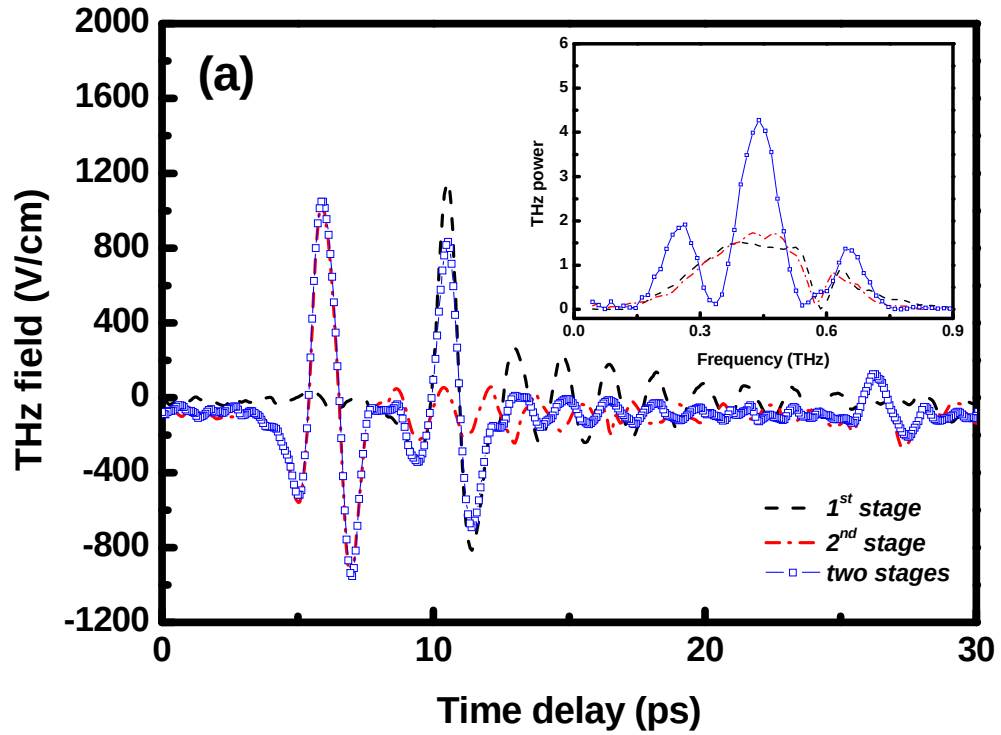
(a)
THz field (V/cm)
Time delay (ps)
THz power
Frequency (THz)
1st stage
2nd stage
two stages

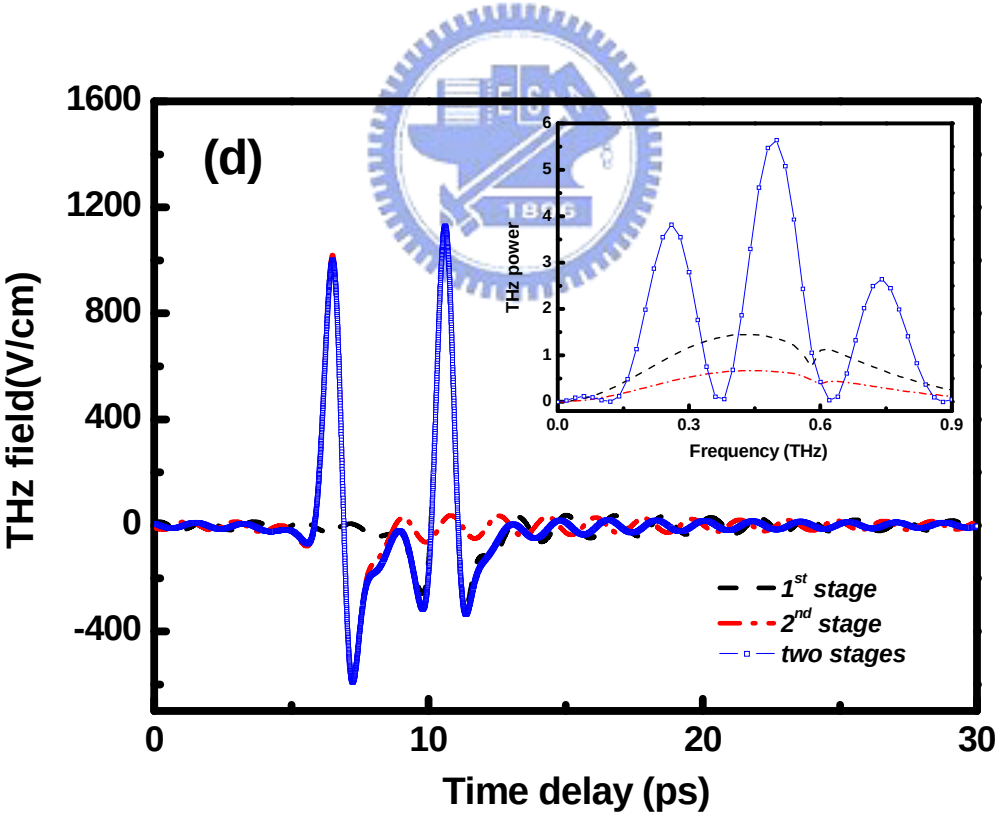
(d)
THz field(V/cm)
Time delay (ps)
THz power
Frequency (THz)
1st stage
2nd stage
two stages

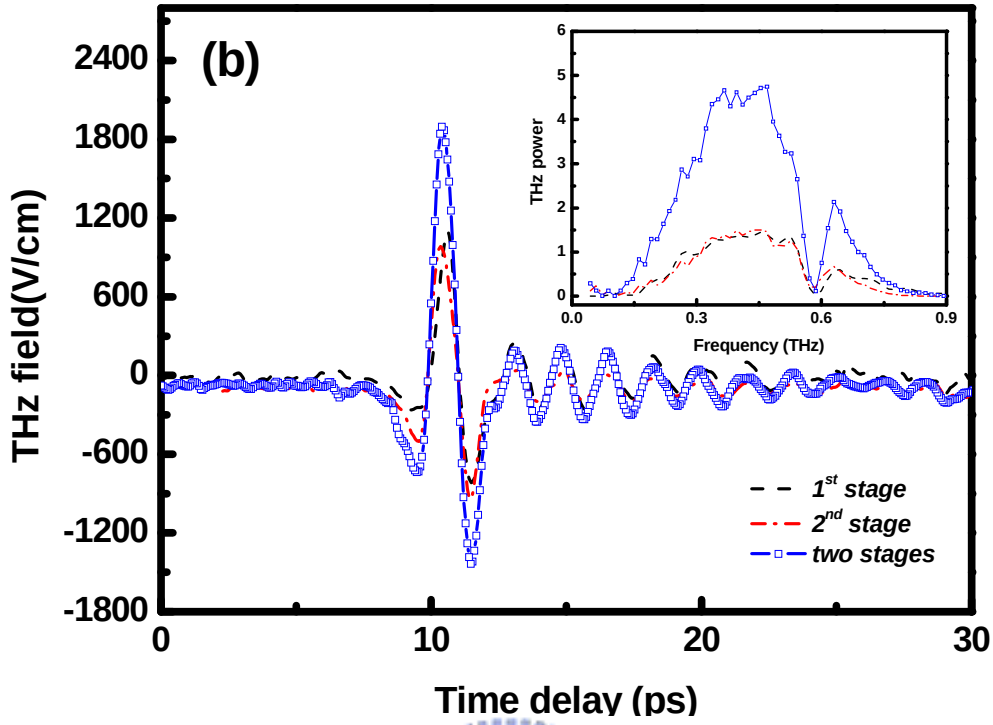
(b)
THz field(V/cm)
Time delay (ps)
THz power
Frequency (THz)
1st stage
2nd stage
two stages

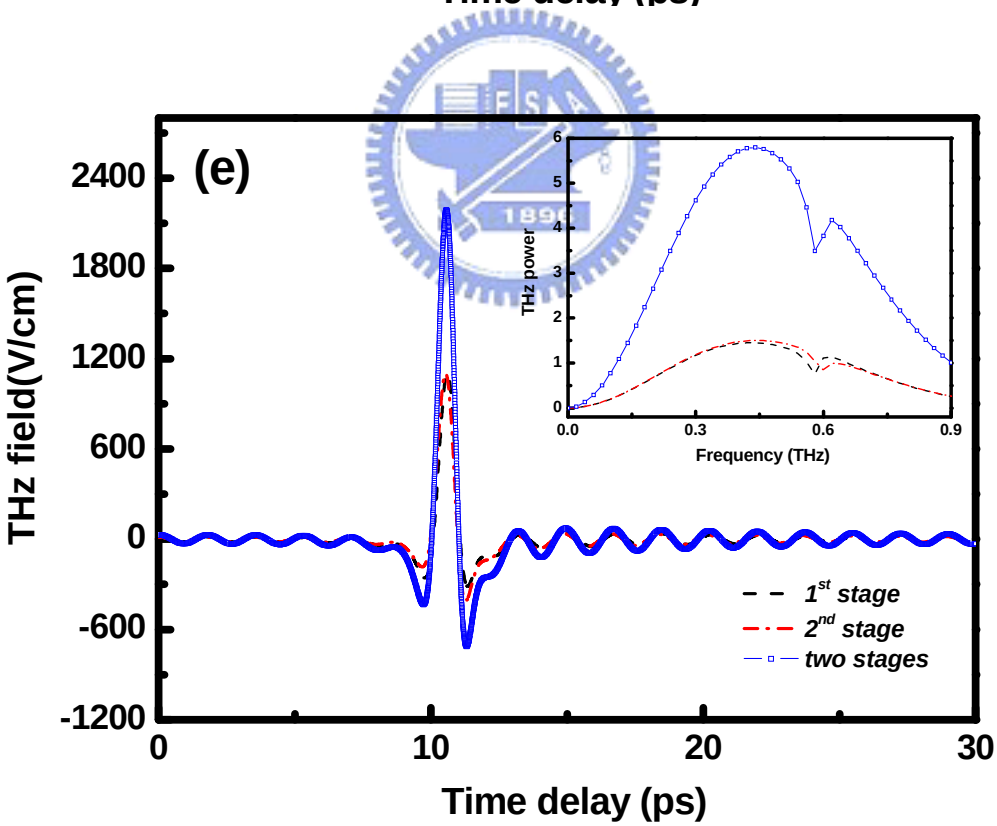
(e)
THz field(V/cm)
Time delay (ps)
THz power
Frequency (THz)
1st stage
2nd stage
two stages

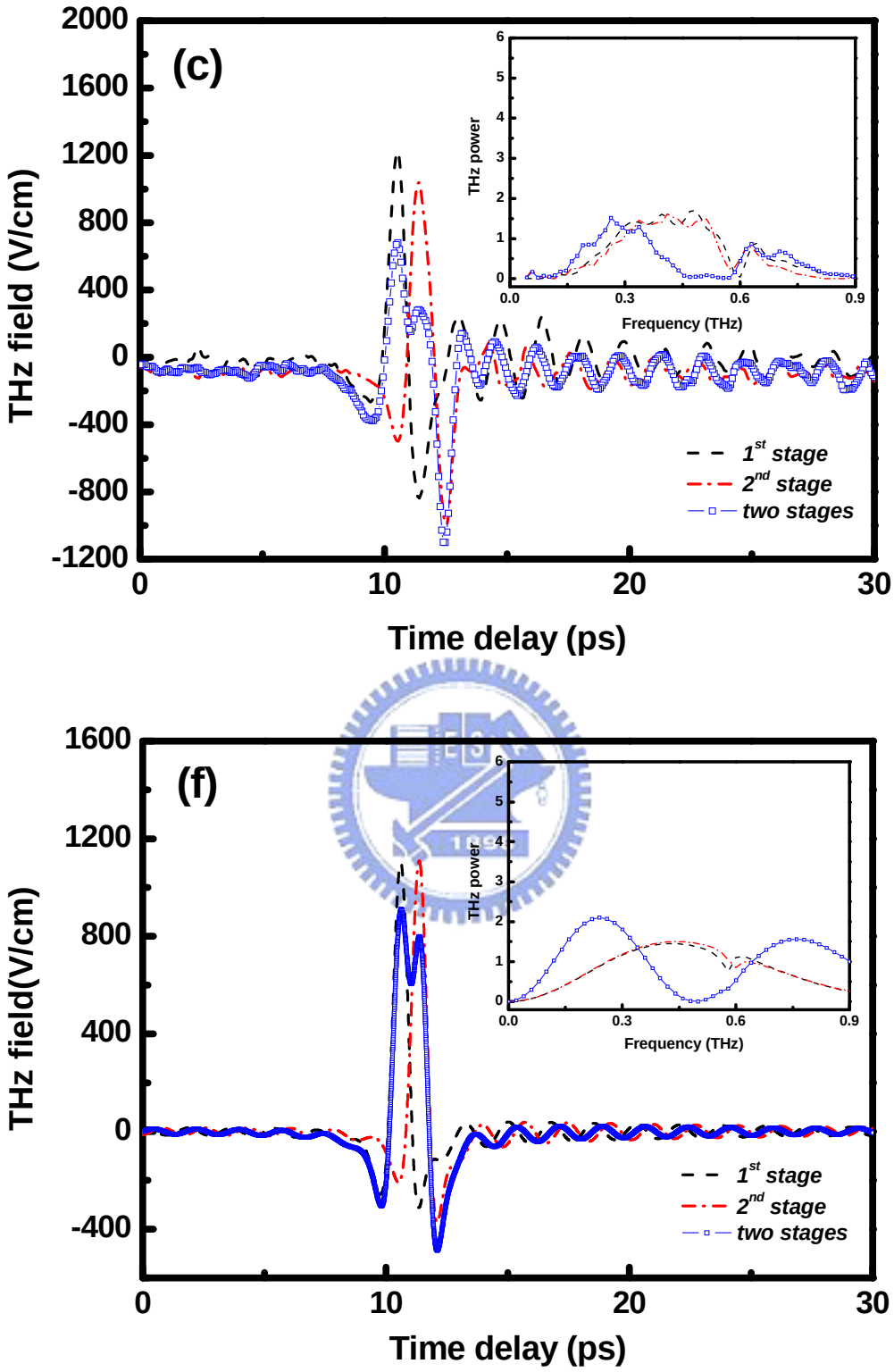

Fig.3-3 Terahertz time-domain waveforms and spectra for three different time delay between the pump pulses of the first and second stages. (a), (b), (c) represent the experimental data at time delay 4.6ps, 0ps, 1ps, respectively. And (d), (e),

(f) depict the theoretical simulation results under same time delay condition corresponding to (a), (b), (c). In (a) and (d), the terahertz pulse from the second stage leads the signal from the first stage; in (b) and (e), the terahertz pulses from the first and second stages are overlapped in the time delay; in (c) and (f), the terahertz pulses from the second stage falls behind that from the first stage. Inset: corresponding spectra of the terahertz radiation.

3.5 Coherence analysis

The Fig. 3-4 (a), (b) and (c) show the magnitude square coherence (MSC) at different time delay corresponding to Fig. 3-3 (a), (b) and (c). The results reveal high coherence between first and second terahertz pulses in the range 0.18~0.82THz.

As the time delay is 4.6ps, coherence is reach to 0.8; while the two terahertz pulses are almost overlapped, coherence is as high as 0.97; the delay is set at 1ps, coherence is also at a high level 0.95. According to these results, by accurately adjusting the time delay, this technique with such a superior property has the potential to make us generate intense power of single cycle terahertz pulse. And through coherent superposition synthesis, it could overcome the limit of walk-off effect from group velocity mismatching. It is notice that coherence lower down due to optical phonon absorption around 0.58 THz .

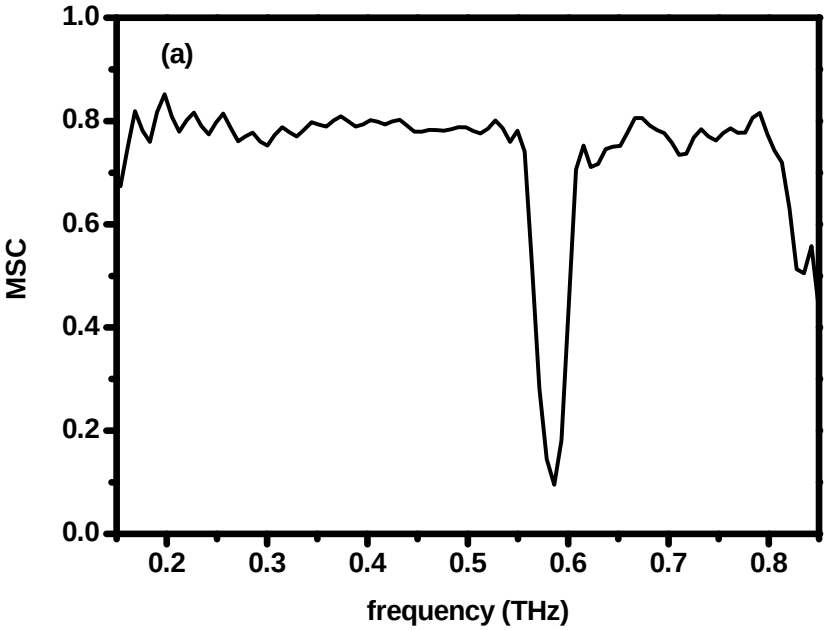
(a)
MSC
frequency (THz)
1.0
0.8
0.6
0.4
0.2
0.0
0.2
0.3
0.4
0.5
0.6
0.7
0.8

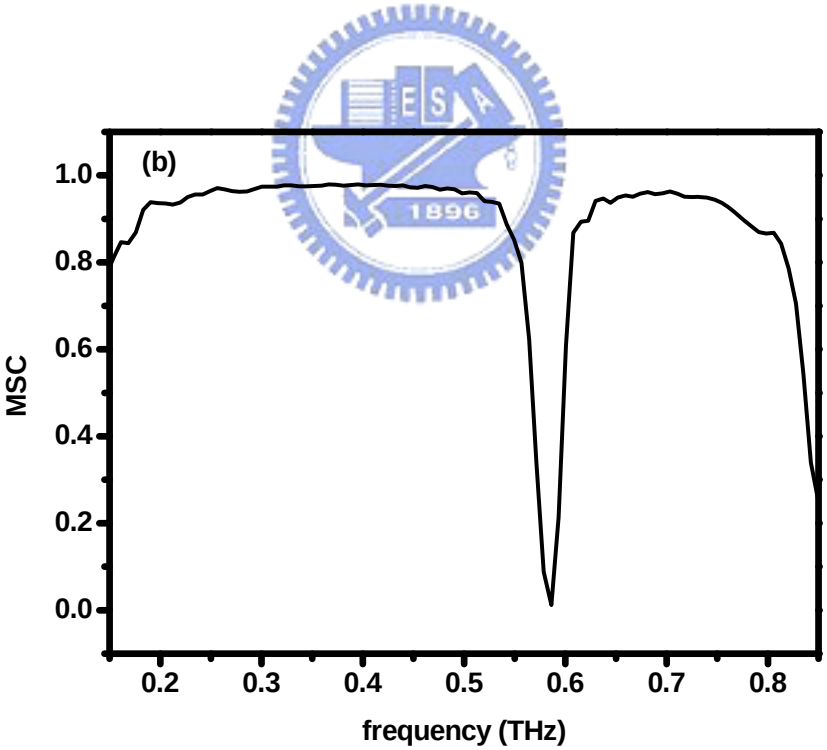
(b)
MSC
frequency (THz)
1.0
0.8
0.6
0.4
0.2
0.0
0.2
0.3
0.4
0.5
0.6
0.7
0.8

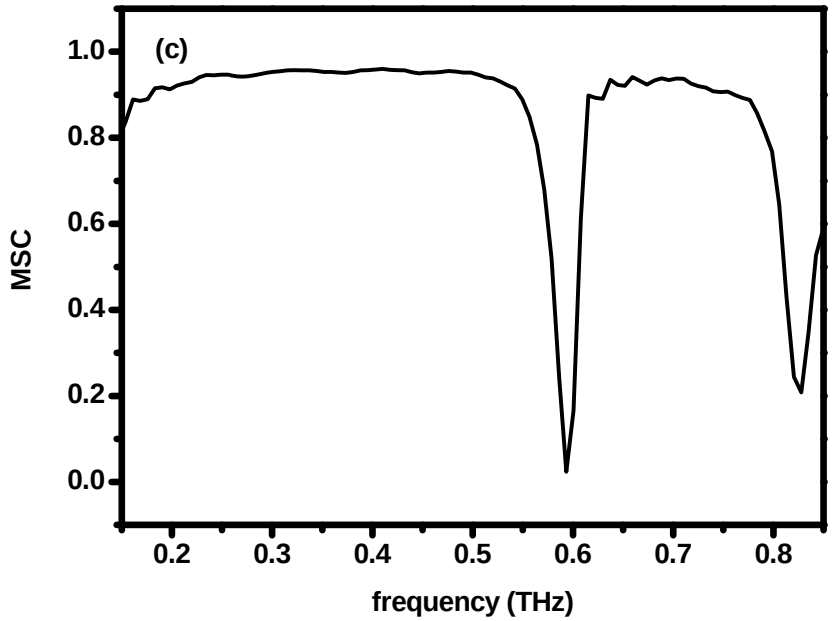

Fig. 3-4 (a), (b), (c) show the MSC corresponding to the Fig. 3-3 (a), (b), (c).

3.6 Summary

Generation of single-cycle terahertz pulses by multiple optical rectification stages using GaSe crystals was proposed and experimentally demonstrated. By properly adjusting the time delay between the pump pulses to the two OR stages, the terahertz radiation field generated by the second stage can be constructively superposed to the seeding terahertz field from the first stage. The high coherence between the two terahertz radiation fields is ensured with coherent optical rectification process and could be further used to synthesize a desired spectral profile of output coherent THz radiation.

Reference

[1] T. Hattori and K. Takeuchi, “Simulation study on cascaded terahertz pulse generation in electro-optic crystals,” Opt. Express 15, 8076-8093 (2007).

[2] G. C. Carter, C. H. Knapp, and A. H. Nuttall, “Estimation of the magnitude squared coherence function via overlapped fast Fourier transform processing,” IEEE Trans. Audio Electroacoust., vol. AU-21, no. 4, pp.337-344,1973.

[3] Benesty, J. Jingdong Chen Yiteng Huang , “A generalized MVDR spectrum,” Signal Processing Letters, IEEE, 12, 827- 830, 2005.

Chapter 4

The absorption effect of free carriers in terahertz range and the optimization of terahertz light sources

4.1 Two photon absorption effect

The nonlinear absorption in GaSe crystal has been well known, and this effect has significant influences in terahertz field generation process. For the higher intensity near infrared pulse pumping, the free carriers could be generated via two photon absorption. The terahertz field could be attenuated by the absorption of free carriers while propagating inside the crystal. The effect of absorption of free carriers decreases the terahertz power severely. The nonlinear absorption of terahertz could be measured by the arrangement of experiment setup

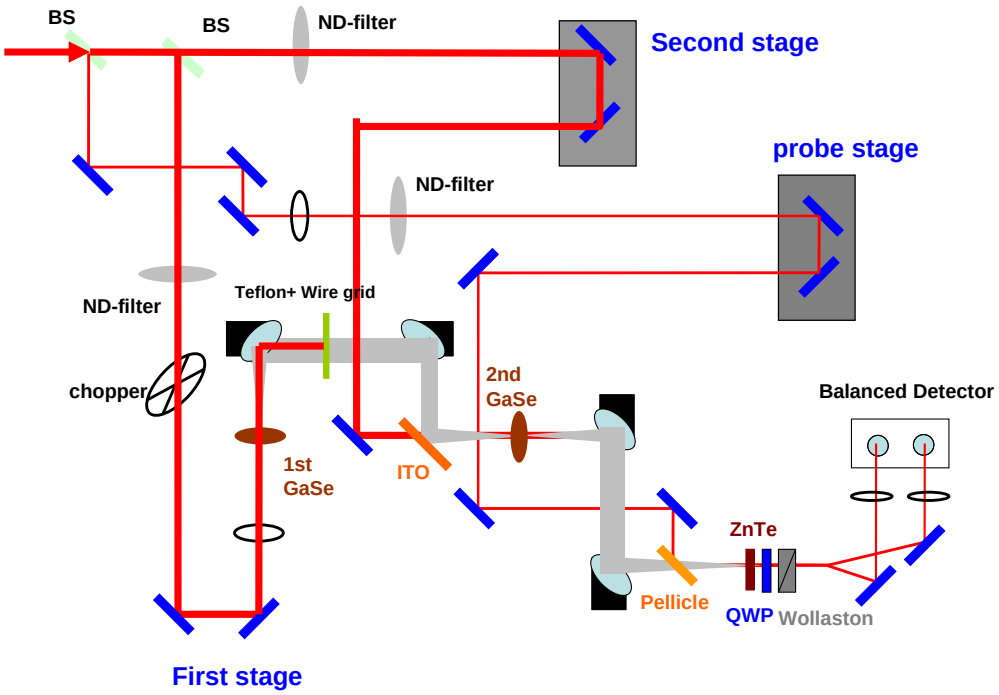

Fig.4-1 Experimental setup. This arrangement could be used to measure nonlinear absorption in THz range.

To access the free carriers absorption effect at terahertz range, we set the optical chopper in the experimental setup at a different position from the multi-stage experiment such that only the gating beam and the first terahertz generation stage could be modulated by the chopper. In such an arrangement, the terahertz field generated by the second stage could not be detected. The experimental setup is shown in Fig. 4-1. We measure the peak amplitude of the terahertz field pulse by varied the optical pump pulse intensity of the second optical rectification stage. The result is shown in Fig. 4-2. Figure 4-2 reveals the measures terahertz field pulse decrease when the optical pump pulse intensity in great than 2 GW/cm^2. The decreasing terahertz field must be caused by free carrier absorption when terahertz pulse and pump pulse co-propagate in the second GaSe crystal.

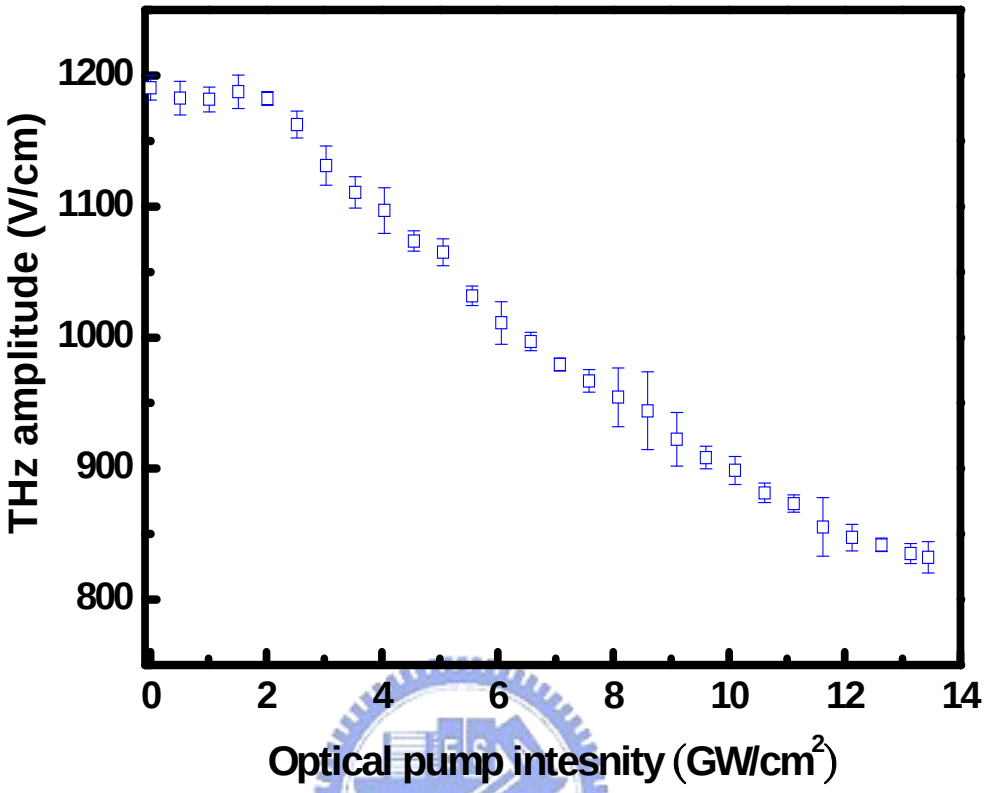

Fig.4-2 Terahertz radiation attenuation by the GaSe crystal under high intensity pump laser pulses.

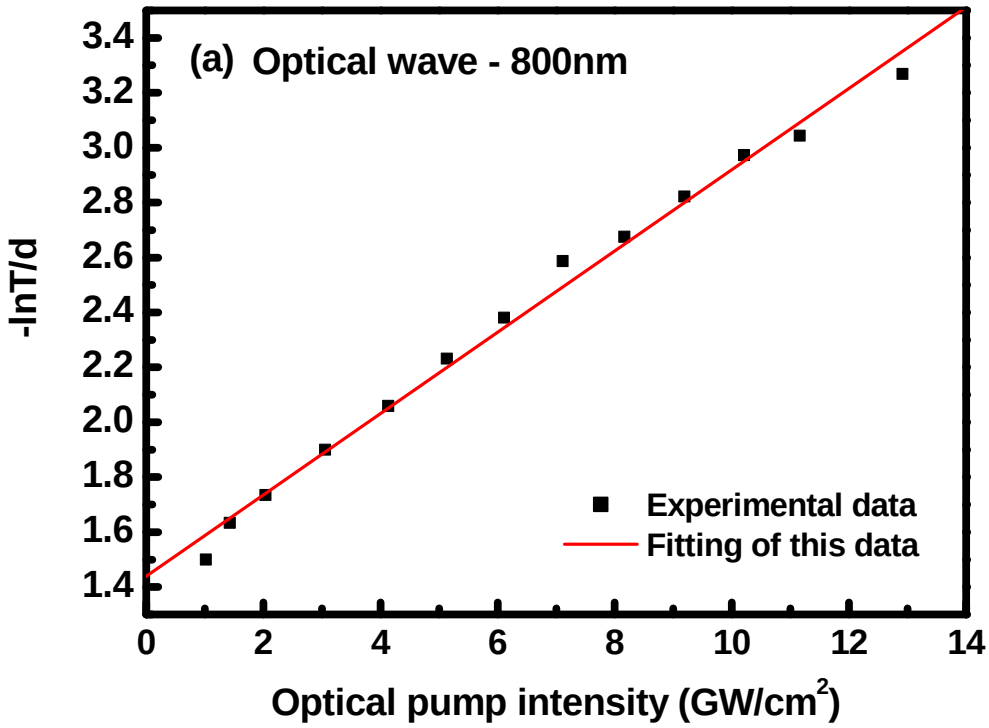

Fig.4-3 Fitting of the experimental data for linear and nonlinear absorption coefficient of GaSe crystal pumped by 800 nm optical pulses.

The absorption coefficients of the optical pump at 800nm in GaSe by linear absorption and nonlinear two-photon absorption are calculated to be α=1.44 cm^{-1} and β=1.48×10^{-10} cm/W, respectively. The results are shown in Fig. 4-3.

From the measurement, we fit the experimental data for the absorption coefficient. According the fitting result, we could estimate the number density of free carriers N in GaSe crystal by the [1][2][3]

$$N = [\frac{F'}{\hbar\omega}](\alpha + \beta \frac{F'}{\tau_p 2\sqrt{2}\sqrt{\pi}}), \quad (1)$$

Here $F' = F_0(1-R)$, F_0 is the energy density of the optical excitation, and the photon energy for optical pump $(\lambda = 800nm)$, $\hbar\omega = 1.55eV$, the optical Fresnel loss at $800nm$ is 0.23, the pump pulse with pulse width full width half maximum is

$\tau_p = \tau_{FWHM} / 2\sqrt{\ln 2}$. In our experimental condition, under the energy density $F_0 = 10GW/cm^2$, the number density of electron-hole pairs are estimated to be $N = 1.5 \times 10^{16} cm^{-3}$.

The absorption of terahertz field pulse by the free carriers generated via two photon absorption in GaSe at high optical excitation level could be calculated by

$$T = \frac{I}{I_0} = \exp(-\alpha_{THz,fc} d) \tag{2}$$

Where I_0 and I express the terahertz intensity before and after the GaSe crystal under the experiment. d is the crystal thickness, and $\alpha_{THz,fc}$ denote the absorption coefficient at terahertz frequency, which is defined as

$$\alpha_{THz,fc} = \sigma_{THz} N . \tag{3}$$

Here the N is the free carrier density under experimental condition and σ_{THz} denotes the absorption cross-section of GaSe at terahertz frequency in the presence of free carrier effect. We could determine the absorption cross section σ_{THz} by fitting the measured data to Eq. (1)-(3), and the results are presented in Fig. 4-4. The fitting result of σ_{THz} lies in the range of $(1.3-5.9)\times 10^{-17}\ cm^2$.

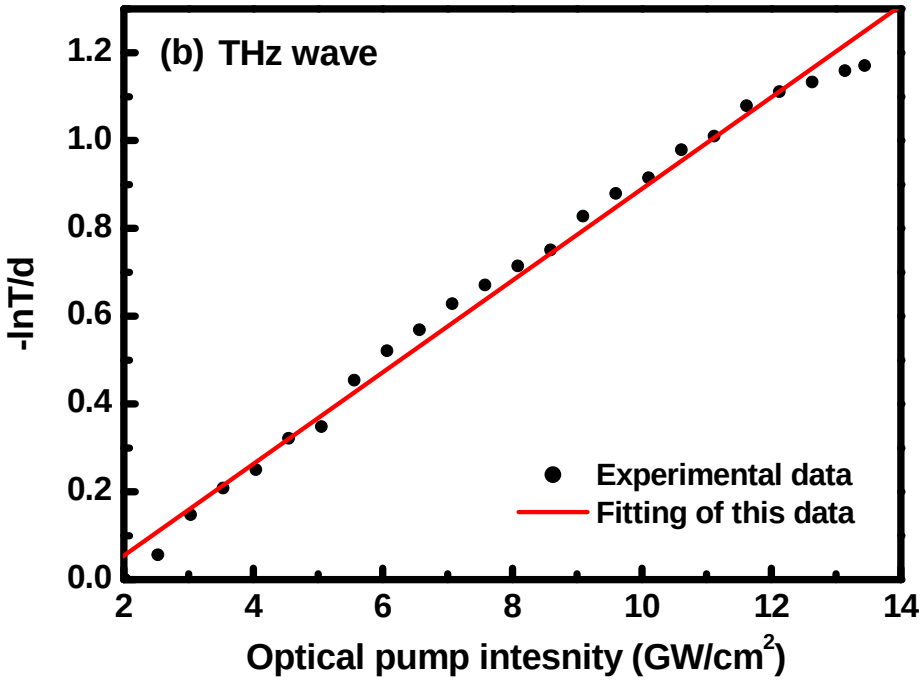

Fig.4-4. Fitting of the experimental data for the absorption coefficient $\alpha_{THz,fc}$ at terahertz frequency in GaSe crystal due to free carriers.

4.2 Pump power and absorption dependence of the THz wave output

Next we study the power dependence of the terahertz field pulse. In this experiment, we block the pump beam at first stage so that the first stage will not generate terahertz field signal. And we make the terahertz generated via optical rectification only in second stage. Also we rearrange the optical chopper to modulate the second pump beam and gating beam simultaneously. Fig. 4-5 shows the main peak of terahertz field radiation output from the second optical rectification stage without the terahertz from the first stage as a function of optical pump intensity.

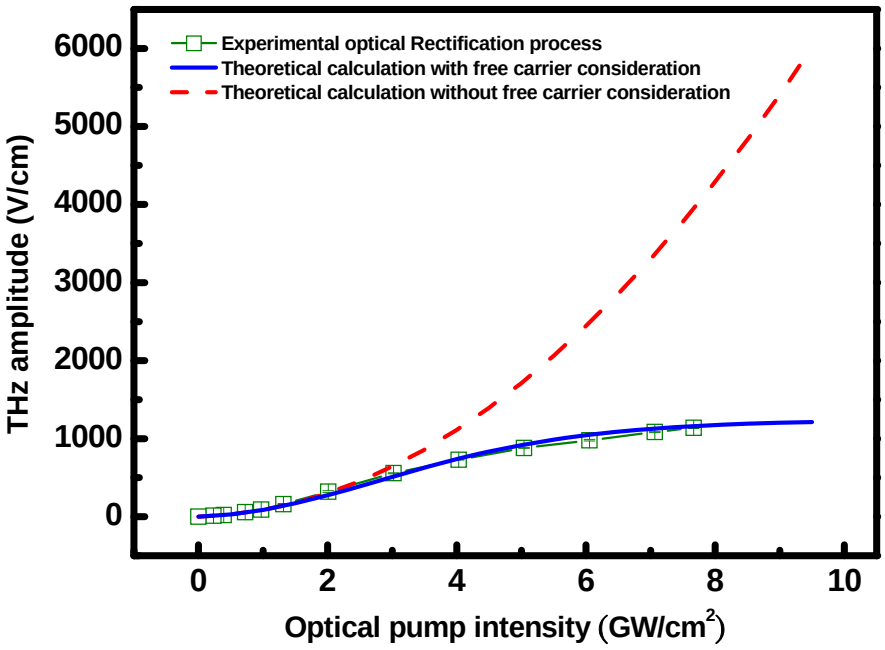

Fig.4-5 Peak field amplitudes of the terahertz pulse at the output of the second OR stage are plotted as a function of pump intensity. Red and blue curves are theoretical predictions without and with the free-carrier absorption taken into account.

At low intensity which is below the 2 GW/cm^2, the main peak of terahertz is almost linear dependent on optical pump intensity, in other words, the terahertz is proportional to square of the optical pump field. This physical phenomenon is agreement with theory of nonlinear theory of three wave mixing. As the optical pump intensity increasing, the peak of terahertz field reveals a slightly nonlinear dependent trend. When the optical pump intensity is above 2 GW/cm^2, a sub-linear dependence is found. This trend of curve due to the absorption of terahertz radiation by the free carriers generated via two photon absorption by the pump pulses at 800nm. When the optical pump pulse intensity is getting much higher, saturation of terahertz field could be seen. The contribution of this physical mechanism is two-photon absorption. The

loss of the optical pump pulse energy due to two photon absorption and absorption of terahertz field by the free carriers generated by the two photon absorption can limit the achievable level of terahertz power.

Also we model the optical rectification generated terahertz radiation with Eqs. (1)-(3). The calculation results are re-scaled properly in order to compare with the experimental data. The red curve in Fig. 4-5 reveals the terahertz output by taking into account the linear optical absorption effect only. The terahertz output increases significantly with the optical pump intensity. The terahertz is almost proportional to the square of optical pump field. Next, we use the parameter of fitting result in previous section, and take free carrier generation from both the linear and nonlinear two photon absorption into account in calculation. The result is also presented in blue curve in Fig. 4-5. The terahertz output saturates at high pump intensity. The calculation result is agreeing well with the experimental data. The free carrier absorption effect limit the terahertz upper level and limit the pump intensity at higher pumping level.

Power saturation of the terahertz radiation from GaSe crystal at high pumping level had also been reported and was attributed to two-photon absorption of the optical excitation beam. The limitation on terahertz radiation output by two-photon absorption can be avoided with lower excitation level by using larger beam size. The generation of high power terahertz radiation is therefore limited only by the finite interaction length of nonlinear optical process used.

To avoid the absorption effect of free carriers in terahertz generated via optical rectification, a possible solution for this problem is lowering the two photon absorption cross section, in other words, using other crystals. The others methods to obtain intense terahertz pulses using electro-optic crystal are based on reduction of

absorption by lowering the temperature of the crystal or change the shape of pump field pulse.

4.3 Significant factor: conversion efficiency

In three wave mixing of nonlinear theory, the terahertz power is proportional to optical pump intensity in the limit of zero absorption. In practical case, in the higher optical intensity, the absorption of free carrier decreases the terahertz power and lowers the nonlinear conversion efficiency severely. For the higher conversion efficiency, we need a longer crystal, in other words, the effective interaction distance.

The interaction length of crystal is another dominated parameter of conversion efficiency. However, improving the generation efficiency of terahertz field pulse with increasing crystal length encounters some difficulties. First, it is very difficult to grow long GaSe crystals with good optical quality [4][5]. Second, the pulse walk off effect between optical pump pulse and terahertz pulse form the group velocity mismatching limits the effective interaction length in the nonlinear process. This effect dominates the useful length of GaSe crystal.

4.4 Simulation results

In order to obtain higher power terahertz pulse, we need to do is optimizing the terahertz generation system and parameters in optical rectification process.

Here, we choose changing optical pump shape as the way to solve this problem. And to obtain a higher terahertz pulse power and maximum conversion efficiency, the beam diameter around 7-mm which is the maximum aperture of crystal is set. Our laser source, the Spitfire, in photon factory (NCTU), could be operated under 10Hz repetition rate, at 800nm central wavelength, pulse duration about 50fs. The laser

pulse energy could be as high as 15 mJ. We take 5 mJ for single stage as pumping source. We demonstrate the total terahertz energy and conversion efficiency by numerical simulation. The crystal length, linear absorption and nonlinear absorption of free carriers are included.

Figure 4-6(a), (b), (c) and (d) show the conversion efficiency and total terahertz energy versus optical pump intensity in different pulse width. Numerical simulation shows the pulse width and effective length could dominate terahertz pulse output energy. The competition between generation and absorption, including linear and nonlinear, yields the conversion efficiency variation. Typically, conversion efficiency lies in the range of 10^{-6}~10^{-4}[6][7]. This value is well agreement with other group. From Figs. 4-6(a), (b), (c) and (d), we could observe that as the pump intensity increasing the conversion efficiency grows high and the narrower pulse width leads to a better result. Unfortunately, the crystal threshold damage is around 20~30 GW/cm^2, the maximum single cycle terahertz field pulse is also with a upper limited threshold, according to the chemical bonding of crystal.

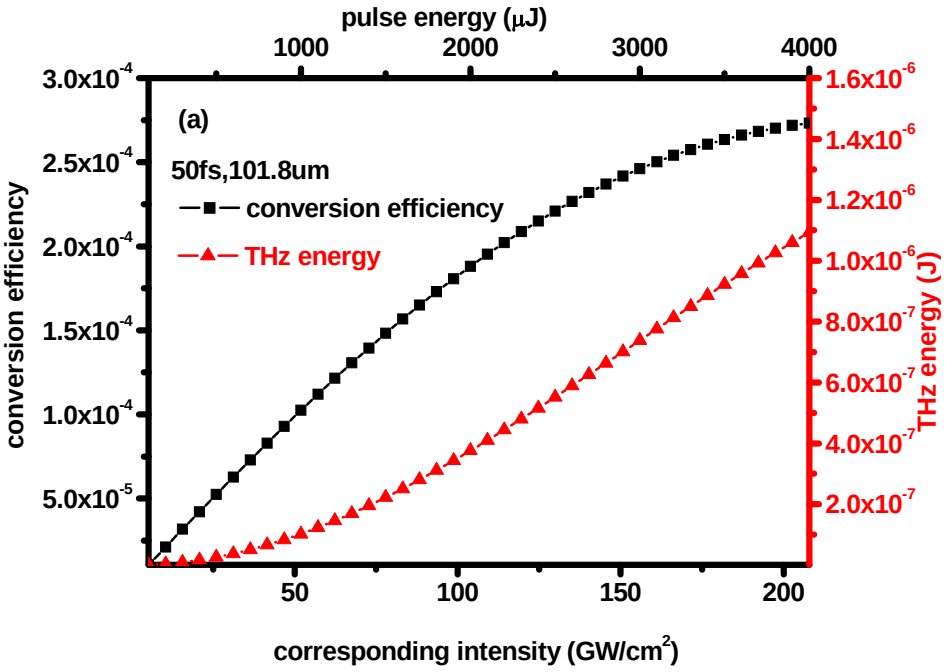
pulse energy (μJ)
1000
2000
3000
4000
(a)
50fs,101.8um
conversion efficiency
THz energy
conversion efficiency
THz energy (J)
3.0x10-4
2.5x10-4
2.0x10-4
1.5x10-4
1.0x10-4
5.0x10-5
1.6x10-6
1.4x10-6
1.2x10-6
1.0x10-6
8.0x10-7
6.0x10-7
4.0x10-7
2.0x10-7
50
100
150
200
corresponding intensity (GW/cm2)

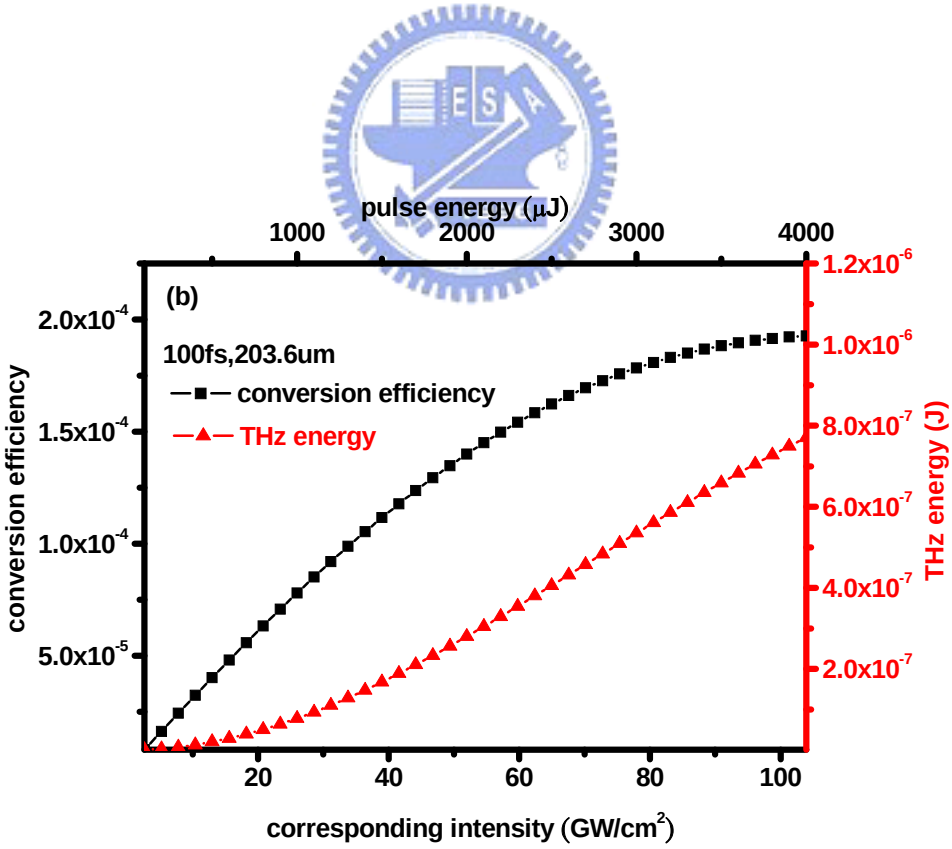
pulse energy (μJ)
1000
2000
3000
4000
(b)
100fs,203.6um
conversion efficiency
THz energy
conversion efficiency
THz energy (J)
2.0x10-4
1.5x10-4
1.0x10-4
5.0x10-5
1.2x10-6
1.0x10-6
8.0x10-7
6.0x10-7
4.0x10-7
2.0x10-7
20
40
60
80
100
corresponding intensity (GW/cm2)

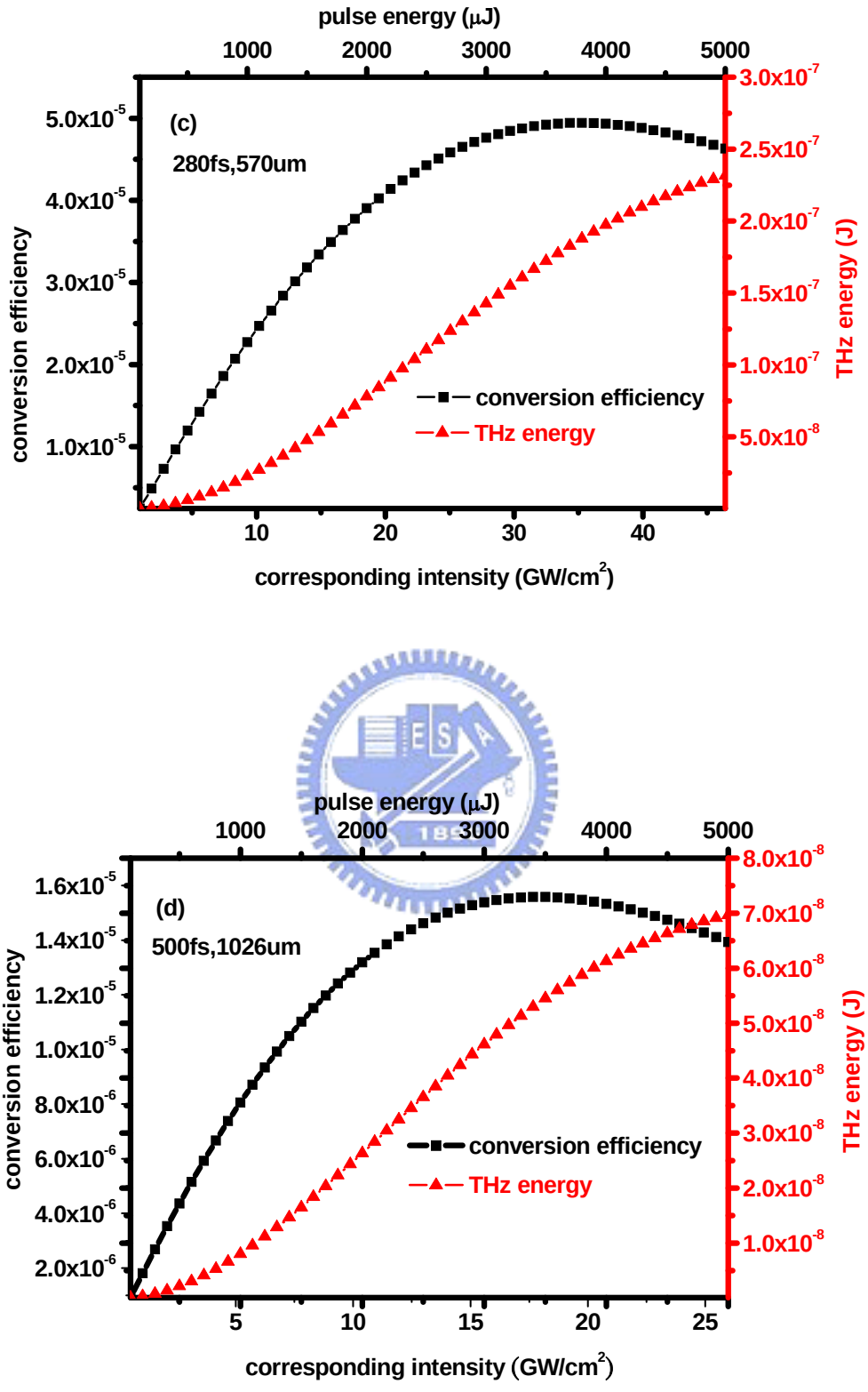

Fig.4-6 (a), (b), (c), (d) show the conversion efficiency and THz energy v.s pump intensity at different pulse width condition and interaction length.

With our laser system, the optimized condition in single cycle is that pulse width equals to 193 fs, with 407 μm crystal propagation distance, below damage threshold corresponding intensity about 25 GW/cm^2. The Fig. 4-7 shows the optimize simulation result. Around the threshold damage, the conversion efficiency is 6.2×10^{-5} and corresponding THz energy is about 133.6 nJ. This result shows the potential of coherent cascaded superposition could be generate to sub-micro joule.

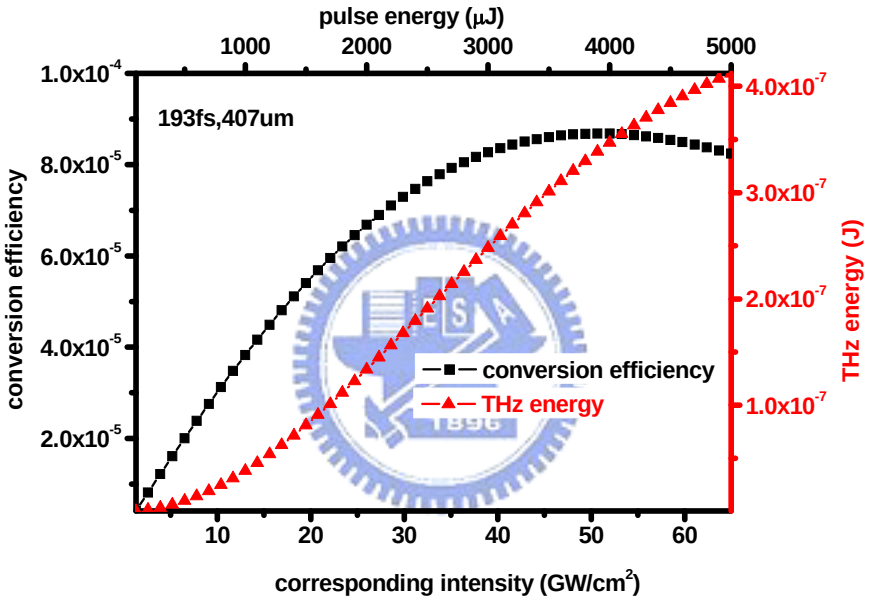

Fig.4-7 The best condition for THz conversion efficiency.

After the Simulation calculation, a design case is proposed to achieve the maximum terahertz output form this technique. The schematic is depicted in Fig. 4-8.

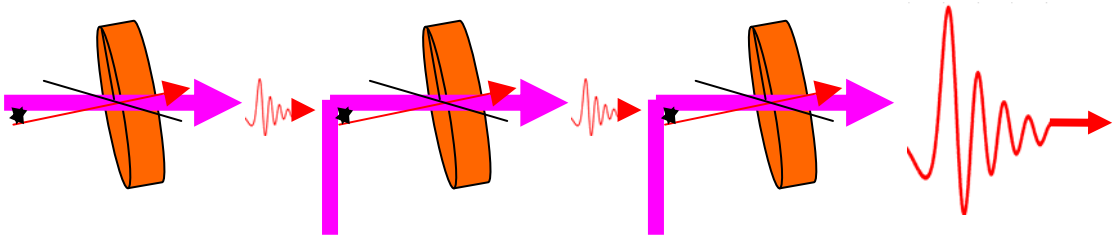

Fig.4-8. The cascaded superposition geometry to generate higher power THz radiation.

According the results in chapter 3, the high coherence between terahertz field pulses radiated from each stage, and considering this simple calculation and design, we predict that the maximum energy output of the terahertz field pulse from the multiple stage optical rectification system.

The total laser pulse energy is divided to three parts for the three-stage optical rectifications. The pulse duration is stretched to 193 fs, focusing spot size is about 7-mm, and each stage GaSe crystal length is 407 μm for each stage. The Fig.4-8 shows the geometry of design case. It is assumed the terahertz wave could be collimated and we neglect diffraction effect.

By accurately adjusting the time delay and making the terahertz radiation cascaded superposition, the output terahertz pulse energy could be as high as 400.8nJ.

4.5 Summary

We demonstrated the numerical simulations about multi-stage of optical rectification in GaSe crystals, and conduct a experimentally approach which generated higher power terahertz pulse radiation. After the coherent superposition of terahertz electric fields in the time domain, the intense single-cycle terahertz pulse could be yielded. Therefore, in our prediction, the maximum pulse energy of terahertz

radiation output by means of the cascaded multiple stage optical rectification is as high as 400.8 nJ.

Reference

[1] I. B. Zotova, and Y. J. Ding, "Spectral measurements of two-photon absorption coefficients for CdSe and GaSe crystals," Appl. Opt. 40, 6654-6658 (2001).

[2] K. L. Vodopyanov, S. B. Mirov, V. G. Voevodin, P. G. Schunemann, "Two-photon absorption in GaSe and $CdGeAs_2$," Opt. Commmun, 155 (1998) 47.

[3] A.M. Kulibekov, K. Allakhverdiev, D.A. Guseinova, E.Yu. Salaev and O. Baran, "Optical absorption in GaSe under high-density ultrashort laser pulses." Opt. Commmun. **239** (2004), pp. 193-198.

[4] N.B. Singh, R. Narayanan, A.X. Zhao, V. Balakrishna, R.H. Hopkins, D.R. Suhre, N.C. Fernelius, F.K. Hopkins and D.E. Zelmon "Bridgman growth of GaSe crystals for nonlinear optical applications,"Mater. Sci. Eng. B **49** (1997), p. 243.

[5] Guoming Z.; Fornstedt T.; Guiochon G.; Singh N.B.[1]; Henningsen T.; Balakrishna V.; Suhre D.R.; Fernelius N.; Hopkins F.K.; Zelmon D.E. "Growth and characterization of gallium selenide crystals for far-infrared conversion applications," Journal of Crystal Growth, Vol.163, No.4, June (1996) , pp. 398-402(5)

[6] T. J. Carrig, G. Rodriguez, T. S. Clement, A. J. Taylor, and K. R. Stewart, "Scaling of terahertz radiation via optical rectification in electro-optic crystals," Appl. Phys. Lett. 66, 121-123 (1995).

[7] Y. J. Ding, "Efficient generation of high-power quasi-single-cycle terahertz pulses from a single infrared beam in a second-order nonlinear medium," Opt. Lett. 29, 2650-2652 (2004).

Chapter 5

Conclusion and future work

5.1 Conclusion

We construct a THz-TDS system and generate single-cycle THz field pulse based on nonlinear optical rectification via nonlinear optical crystal of GaSe, and detect through EO-sampling technique. The effective nonlinearity dependence could be observed by altering the azimuthal angle of GaSe crystal.

Furthermore, the single-cycle terahertz field pulse by multiple stages optical rectification by use of GaSe crystal is demonstrated. By adjusting the suitable time delay between the two terahertz field pulses, the output of terahertz radiation could be constructively cascaded superposition and with higher output power.

The high mutual coherence in the range 0.18~0.82THz between the two terahertz pulse is also reported. As the time delay is 4.6ps, coherence is reach to 0.8; while the two terahertz pulses are almost overlapped, coherence is as high as 0.97; and the delay is set at 1ps, coherence is also high as 0.95. According to this high coherence, this technique has the potential to generate intense power of terahertz pulse which is not limited by the pulses walk-off effect from group velocity mismatching.

Besides, we calculate the nonlinear absorption cross section coefficient in the terahertz frequency range in GaSe crystal, which lies in the range of $(1.3-5.9)\times10^{-17}$ cm^2.

Moreover, a simple design case of cascaded multiple stages of optical rectification is proposed. It is simulated that terahertz energy and conversion efficiency from the laser source with repetition rate at 10 Hz, central wavelength at 800 nm, 50 fs. The used laser pulse energy could be as high as 15 mJ. From the numerical simulation, we expect to achieve the sub micro-joule terahertz energy output from this technique.

5.2 Recommendation and future work

For a better performance of system, it should be enclosed in the dry nitrogen purged and cooled to reduce the free carrier absorption effect.

Two-photon absorption and nonlinear refraction index could severely limit the maximum THz conversion efficiency in the OR or DFG process. The pump beam will create free carriers which strongly absorb THz radiation nonlinear refraction index, on the other hand, which affects the pump pulse itself via self-phase modulation and self –focusing.

It is very advantageous to use longer pump wavelength to avoid two photon absorption effects which are usually strong in semiconductors for near infrared pump pulse. The cascaded system could be designed as three stages and the total pulse energy is also divided into three parts for the pumping source. The pulse width is recommended to stretch to ~193 fs and beam size on crystal surface is around 7-mm, each stage with the crystal length ~407 μm. The maximum conversion efficiency is about 6.2×10^{-5} for each stage below the threshold damage. After cascaded coherent superposition of optical rectification, in the simulation, the maximum single-cycle pulse energy of terahertz light source could be up to 400.8 nJ.